VOL. 6 NO. 2 December 2020

JOURNAL OF NETWORK OPERATIONS

SCTE • ISBE STANDARDS

NETWORK OPERATIONS

scte.org • isbe.org

NETWORK OPERATIONS

SCTE · ISBE

Society of Cable Telecommunications Engineers
International Society of Broadband Experts

JOURNAL OF NETWORK OPERATIONS

VOLUME 6, NUMBER 2
December 2020

Society of Cable Telecommunications Engineers, Inc.
International Society of Broadband Experts™
140 Philips Road, Exton, PA 19341-1318

© 2020 Society of Cable Telecommunications Engineers, Inc. All rights reserved.

SCTE · ISBE STANDARDS

Table of Contents

Editorial Correspondence: If there are errors or omissions to the information provided in this journal, corrections may be sent to our editorial department. Address to: SCTE Journals, SCTE•ISBE, 140 Philips Road, Exton, PA 19341-1318 or email journals@scte.org.

Accepted Submissions: If you have ideas or topics for future journal articles, please let us know. Topics must be relevant to our membership and fall under the technologies covered by each respective journal. All submissions will be peer reviewed and published at the discretion of SCTE•ISBE. Electronic submissions are preferred, and should be submitted to SCTE Journals, SCTE•ISBE, 140 Philips Road, Exton, PA 19341-1318 or email journals@scte.org.

Subscriptions: Access to technical journals is a benefit of SCTE•ISBE Membership. Nonmembers can join at www.scte.org/join.

From the Editors

Welcome to Volume 6 Issue 2 of the *Journal of Network Operations*, a publication of collected papers by the Society of Cable Telecommunications Engineers (SCTE) and its global arm, the International Society of Broadband Experts (ISBE).

The previous issue of this *Journal*, Volume 6, Issue 1, included papers related to what we described as "A relatively new tool in the cable network architecture toolbox … known as distributed CCAP architecture (DCA), which includes remote PHY and remote MACPHY – the latter … called flexible MAC architecture." Also referred to as distributed access architecture (DAA), the technology allows operators to relocate some headend or hub site functionality to nodes or elsewhere. For example, the subset of DCA/DAA known as remote PHY (R-PHY) moves the physical layer electronics to shelves and nodes, while keeping the MAC layer electronics in the headend or hub. A module or circuit called a remote PHY device (RPD) is installed in the shelf or node, and is connected to the headend or hub using a digital fiber link such as 10 gigabit Ethernet.

The RPDs in the nodes essentially replace racks of headend/hub downstream modulators, upstream demodulators, and other RF signal sources and receivers. At first glance one might think that a key benefit is reducing rack space, powering, and HVAC requirements. To some degree that's true, but connecting all of this together is a converged interconnect network (CIN), which means that some types of equipment are replaced by other types. A key benefit to DCA/DAA is the improved signal quality that is a result of using digital fiber links instead of legacy analog optical links. For more about the benefits of DCA/DAA, see https://www.cablelabs.com/technologies/distributed-access-architecture.

So, it's no surprise that in this issue RPDs are a key topic, especially when it comes to how many of them will be needed in network upgrades. In "Operational Transformation in the Design of the Access Network Through Automation and Optimization" Ian Oliver reports on an artificial intelligence (AI) tool that reduces network upgrade design time to a third of manual design time and also provides a 15% reduction in capital costs for network upgrades. The capital costs were shown by Oliver in a previous SCTE *Journal of Energy Management* paper to lead to energy savings via reducing the number of new outside plant (OSP) devices. Such a tool thus holds promise for further savings if, as we suspect, the constraints of coax energy losses from suboptimum power supply locations, along with permitting costs (and delays!) from moving power supplies can be added to the AI algorithms. This could become quite a tool for cable operators as they continuously upgrade their OSP networks!

Also targeting better tools for cost reductions in OSP network upgrades in this issue is Dr. Franklin Lartey of Cox. If one candidate network upgrade design resulted in 1.0 million ± 10% new RPDs required, while another design predicted 1.01 million ± 1%, which would you choose? The latter has a slightly higher mean value predicted, but with much lower uncertainty in that estimate, so it has a lower maximum possible value of RPDs required. Intrigued? Then check out Lartey's paper "Predicting the Number of Remote PHY Devices in a Hybrid Fiber/Coax Node+0 Deployment" on using Uncertainty Reduction Theory (URT) to more precisely estimate the number of RPDs required. You'll also learn how precision in the operator's knowledge of plant mileage, number of current amplifiers, and households passed affects the precision in which capital costs of upgrades can be estimated.

A third paper in this issue covers a topic that has been an important part of cable network maintenance for decades: broadband sweeping. “Developments in Cable Network Frequency Response Characterization” was penned by one of us (Hranac), who climbed poles and did sweep testing and plant alignment in a past life using many of the instruments mentioned in the paper. The paper includes a comprehensive overview of the technology used for measuring cable network and individual channel frequency response, from the 1960s through the present. The current state of the art is discussed, as are the benefits of sweep testing. Indeed, Ron notes in the paper, “As long as RF is present in cable networks, sweeping should be considered an important part of network maintenance.”

We are grateful for the individuals who contributed to the *Journal of Network Operations*, including the authors, reviewers, and the SCTE·ISBE publications and marketing staff. We hope you enjoy this issue of the *Journal*, and that the selected papers provide inspiration for new ideas and innovations in cable network operation. If you have feedback on this issue, have a new idea, or would like to share a success story please let us know at journals@scte.org.

SCTE·ISBE *Journal of Network Operations* Senior Editors,

Ron Hranac (Retired)

SCTE•ISBE Fellow Member

Daniel Howard

Principal, Enunciant LLC.

SCTE•ISBE Senior Member

Operational Transformation In The Design Of The Access Network Through Automation And Optimization

Findings from Pilot Deployments

A Technical Paper prepared for SCTE•ISBE by

Ian Oliver, President, Versant Solutions Group, SCTE•ISBE Member
21 Radford Crescent
Markham, Ontario, Canada L3P 4A2
ian.oliver@versantsolutionsgroup.com
+1 416 543 3360

Table of Contents

List of Figures

List of Tables

1. Introduction

This paper presents and discusses the application of advanced expert system AI, mathematical, and geospatial information processing techniques to the automated production of optimized preliminary designs for the access network. It draws on the findings of pilot deployments of the aforementioned technologies, as incorporated into an integrated platform, at several North American cable operators from 2018 through 2020.

The paper describes how the application of the automated design and optimization platform has fulfilled the fundamental criteria for success – time and cost savings – as well as how it supports the operator in meeting the challenges involved in executing the network upgrades needed to meet constantly growing customer demand. Quantitative findings and results of the pilot deployments are cited to describe the efficacy of the automated design and optimization platform. Furthermore, this paper provides a qualitative synopsis of how operators involved in the pilot deployments see the automated design and optimization platform being transformative to their businesses in the longer term.

2. Operational Context for Application of Automated and Optimized Design of the Access Network

Cable operators are collectively facing an urgent requirement to:

1. Evaluate, select, and deploy multiple access network technology options such as DOCSIS® 4.0, spectrum expansion strategies, upstream frequency splits, FDX, DAA, new amplifier types, and new tap technologies when undertaking network upgrades across their respective footprints;

2. Address the fact that the existing access plant is aging and, while it has been ingeniously pushed to ever-higher levels of performance over the years, is nearing its end-of-life;

3. Undertake access network upgrade projects with a workforce that no longer comprises a strong contingent of experienced outside plant designers and engineers, and that is increasingly likely to be scattered geographically across an operator's footprint and, perhaps, rarely in the physical presence of one-another;

4. Utilize both the fibre distribution network and the coax network in an optimal, holistic manner to service both residential and business customers – and to support and integrate new technologies and services such as those involved in 5G systems;

5. Ensure that the access network powering system provides availability levels comparable to what is provided by power systems in core facilities so that remote PHY and remote MAC/PHY devices in the access plant can provide continuous service to customers, all the while optimizing power supply utilization to meet energy efficiency targets;

6. Accomplish all of the foregoing quickly, at the minimum possible operational and capital costs.

Within a cable company, the primary responsibility for responding to all of these requirements falls upon the technology and engineering personnel, typically including the CTO, technology strategists, network planners and engineers. Historically, the technology and engineering personnel have relied upon manual effort and deep industry experience to respond effectively to demands on the network to support more

services and more bandwidth. Indeed, during the deployment of the first HFC networks in the late 1980s through the early 2000s, that approach was effective and resulted in the deployment of the access network that has enabled massive growth in the industry over the last 20+ years.

However, today's challenges are for more complex than was the case 20 years ago, with operators having to consider multiple physical network architectures (e.g., N+0, N+2, FTTH), and multiple spectrum configurations and transmission technologies (e.g., DOCSIS® 4.0, FDX, ESD). And, senior management requires technology recommendations, complete with cost estimates, that are timely and valid in order to confidently commit millions of dollars in capital to network upgrades.

Additionally, given all of the current technology options and those to come available to the operator, it is increasing likely that there will be no 'one size fits all' option that would be suitable for deployment across an operator's entire footprint. Rather, the author's experience in working with operators in recent years suggests that an operator is likely to implement two or three physical network architectures, all the while operating a combination of DOCSIS 3.0, DOCSIS 3.1, and DOCSIS 4.0 along with corresponding spectrum configurations (*Roaring Into The '20s With 10G;* Howald, Dr. Robert; 2020 SCTE Tec-Expo Proceedings). This reflects an underlying, constant theme: To continue to maximize the performance of the existing coaxial cable network and to maximize the return on capital investment, both past and present, in that network.

In such a context, the technology strategy and network planning personnel can be quickly overwhelmed, resulting in poor decision-making regarding capital investment in network upgrades, further resulting in increased risk of wasted money and lost customers.

In short, it's either a very good time or a very bad time to be a technology strategist or network planner, depending on one's point of view.

3. From Strategy to As-Built, and How Design Automation and Optimization Fits In

The traditional process for making strategic technology and capital expenditure decisions and then realizing such decisions in the form of deployed access networks is shown in Figure 1. While this process has served cable operators well to date, its inherently labour and time intensive nature is causing operators to explore opportunities to automate – and accelerate – the design and cost estimation process in order to reduce the cycle time involved in making strategic technology and capital expenditure decisions from many months to a matter of weeks, if not days.

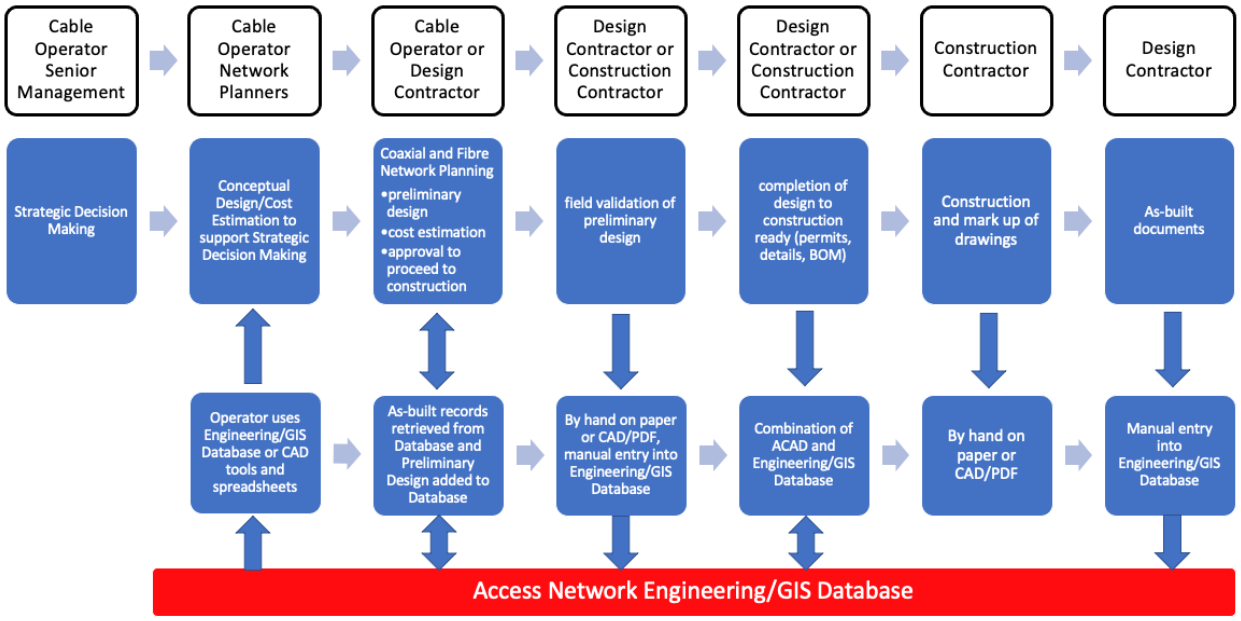

Figure 1 - Traditional Manual Process

In the several pilot deployments undertaken to date, it was demonstrated that the automated design and optimization platform being proven was actually producing designs that were directly comparable to preliminary designs, by virtue of being much more complete than a typical manually produced conceptual design. In particular, the resulting designs:

- Were consistently compliant with the operator's design rules for N+0 and N+2 architectures AND were fully optimized for lowest capital cost;
- Presented fully calculated RF network designs, based on the operator's active and passive equipment and RF cabling, both existing (as retrieved from the engineering/GIS database) and newly placed (as specified by the operator);
- Called for the physical, real-world, location of new equipment, particularly nodes/pedestals, consistent with how an experienced network planner or engineer would do so, for example, avoiding rear lot easements.

All of the foregoing was realized by:

- incorporating the operator's explicit (written) design rules into the automated design engine;
- utilizing advanced software techniques to emulate how experience planners and engineers make decisions on equipment placement;
- reading the existing access network as-built design into the automated design engine and using that as-built design (including the physical support structure, both aerial and buried) as the basis for all new design;
- taking advantage of the speed and sheer computational capability of advanced software techniques and computing hardware to develop and evaluate practically every possible technically valid design in order to deliver the preliminary design having the lowest capital cost estimate.

To summarize, the automation and optimization technology deployed in the pilots **always follows the rules and doesn't stop until the lowest cost preliminary design has been found.**

Interestingly, in an early deployment it was found that the automated design engine was initially producing designs that consistently called for more new nodes than did the manually produced designs for the exact same service areas. Upon examination, it was determined that the planners and engineers responsible for the manually produced designs had done what all good planners and engineers do: They 'cheated' by, quite appropriately, slightly exceeding the specified RF signal level constraints in order to reduce the number (and cost) of new nodes required. Once the automated design engine was configured (allowed, as it were) to similarly 'cheat' where appropriate, the resulting designs were found to be directly comparable to the manually produced ones and, on the whole, calling for significantly fewer new nodes.

As a result of the finding that the automated design and optimization platform actually produces fully detailed preliminary designs, not simply conceptual designs, the traditional strategy-to-implementation process can be modified to be as shown in Figure 2.

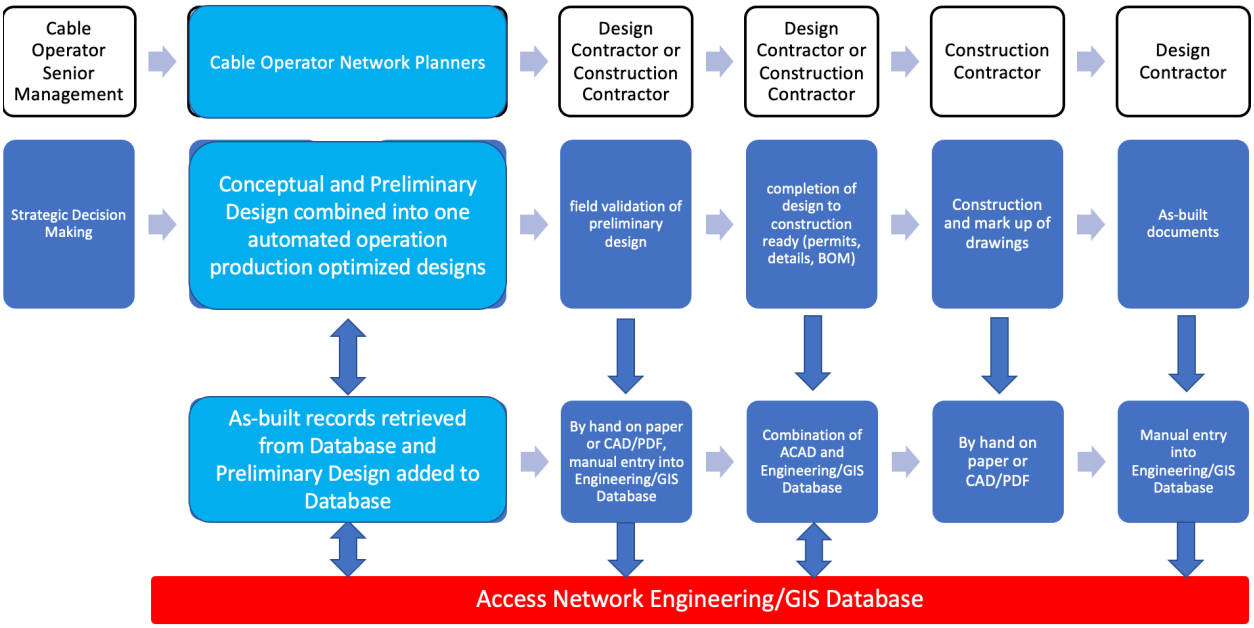

Figure 2 - Automation and Optimization Inserted Into Process

4. Findings From Pilot Deployments

Three pilot deployments were conducted, one each in 2018, 2019, and 2020, with three different North American cable operators. The first one focused on N+0 network architecture, while the remaining two addressed N+2 architecture.

The goal of all three deployments was to demonstrate and confirm the ability of the automation and optimization technology to produce preliminary designs that were optimized for lowest capital cost and, otherwise, directly comparable to what an experienced network planner or engineer would produce, complete with a fully detailed bill-of-materials and construction cost estimates, all suitable for supporting

strategic technology decision making and commitment of capital funding – in far less time than could be accomplished manually.

In all three pilot deployments, the existing node boundaries were respected and all new N+0 and N+2 serving areas were created within the existing node boundaries.

4.1. N+0 Pilot Deployment Findings

This pilot deployment, conducted in 2018, comprised a direct comparison between N+0 architecture preliminary designs as produced by the operator's network planning personnel and as produced by the automated design and optimization platform for 45 existing HFC node serving areas.

The table below summarizes the findings of the pilot deployment and shows, in particular, the financial benefit afforded by the optimization capability of the technology. The cost figures shown in Table 1 are based on the operator's standard unit cost figures for estimating the equipment and construction labour costs for network deployment that, in this case, comprise N+0 nodes and all downstream coaxial cable, splitters and taps. Cost estimates for deployment of fibre cable to serve the N+0 nodes are not included in the figures below.

Table 1 - Summary of Quantitative Analysis of N+0 Pilot Deployment

Design Characteristic	Produced Manually	Produced by Automated Design Tool
Total # of Existing HFC Nodes	45	45
Total # of N+0 Nodes	263	198
Total Metres of New Coax Route	15,910	22,164
Total Cost of N+0 Nodes + Coax	$12,300,000	$10,450,000
Lower Cost to Upgrade to N+0 Architecture	17 of 45 existing HFC nodes	28 of 45 existing HFC nodes
Avg. Cost to Upgrade Exist HFC Node to N+0 Architecture	$275,000	$235,000

Note 1: This table was previously presented in *Optimizing Node+0 Outside Plant Design for Cost and Energy Efficiency Using Artificial Intelligence;* Ian Oliver; 2019 SCTE-ISBE Journal of Energy Management

Additional findings, both quantitative and qualitative, regarding the benefits of utilizing the automated design and optimization platform included:

- Time savings in the production of the preliminary designs whereby the operator's planning personnel calculated that the automated design capability:
  - reduced the time required per existing node area from three person-days to less than one person-day, and;
  - offered further times savings of three person-days by virtue of being able to import the preliminary designs from the automated design engine directly into the engineering/GIS platform, thus eliminating the need for manual entry (i.e., drafting) of the designs in the engineering/GIS environment;
- Previously impossible ability to provide senior management with capital cost estimates for major network upgrade projects in a matter of days and weeks rather than months, with those estimates

being based on actual preliminary designs rather than less accurate estimation techniques (e.g., typical cost-per-home-passed);
- Increased consistency in the application of corporate engineering design standards to all design work by virtue of the design engine "always following the rules";
- Significantly improved effectiveness of the operator's network planning and engineering groups by delegating the rote work of network planning and design to a technology that is ideally suited for such work, thereby freeing up the time of planners and engineers for doing the valuable work that only experienced professionals can do. (One operator's network planners referred to this as 'having an Easy button'.)

4.2. N+2 Pilot Deployments Findings

Two pilot deployments for N+2 network architecture were conducted, one each for two different cable operators. In both pilots, a fundamental design rule was that that new N+2 nodes were to be placed only at locations of existing active devices in the coaxial network, i.e., the location of the original HFC node or an amplifier. The N+2 nodes specified for each pilot provided RF output levels comparable the active devices being replaced, thus maintaining RF performance in the coaxial network. Further, it was assumed that the existing coaxial network was in compliance with the operators' RF performance specifications and, by virtue of being essentially unaltered, would remain in compliance after the placement of new N+2 nodes.

4.2.1. N+2 Pilot Deployment #1

This pilot deployment was conducted in 2019 in order to allow the operator to assess the ability of the automated design and optimization platform to meet its technical and operational requirements for the automated production of preliminary designs for N+2 network architecture in 111 existing HFC nodes. The pilot deployment also included the automated routing of new fibre cable to serve the new N+2 nodes.

At the time of the pilot deployment, the operator was using an entirely manual approach to generating conceptual designs and cost estimates, whereby:

- Technicians manually created N+2 'pockets' within the existing HFC network architecture through visual examination thereof, and recorded the pocket boundaries in a simple, stand-alone mapping tool, and;
- Planners manually generated capital cost estimates by using the quantity of pockets created and the operator's standard unit construction cost figures.

For purpose of evaluation of designs produced by the automated design and optimization platform, the operator chose to consider how much 'better' the optimal N+2 design for each existing node area was relative to all non-optimal N+2 designs for the same node area. This approach was possible because the automated design engine produced **all technically compliant N+2 designs** for each existing node area, then the optimization function determined **which design comprised the lowest construction cost estimate** (using the operator's standard unit construction cost figures).

This evaluation approach was selected by the operator in order to allow it to understand the risk of **not** using the automated design and optimization platform in terms of both increased capital cost for network deployment and increased ongoing costs for network operation – both of which the operator understood to be driven by the quantity of equipment (e.g., nodes) and of cabling (i.e., fibre) comprising the access network.

It was found that there was only one possible optimal design for each existing node, and that that design comprised the lowest number of N+2 nodes **and** the least amount of new fibre cable.

In terms of N+2 node quantity optimization, it was found across **all** existing nodes that:

- The next best designs, i.e., optimal +1, call for 29% more N+2 nodes on average than the optimal design;
- The worst-case designs (optimal + 3, for the most part) call for 96% more N+2 nodes on average than the optimal design.

Similarly, with respect to quantities of new fibre metres, it was found across **all** existing nodes that:

- The next best designs, i.e., optimal +1, call for 38% more new fibre on average than the optimal design;
- The worst-case designs (optimal + 3, for the most part) call for 111% more new fibre on average than the optimal design.

Table 2, below, provides a quantitative analysis of the preliminary designs produced by the automated design and optimization platform.

Table 2 - Cost Analysis for N+2 Designs by Automated Design Engine

	Optimal Designs	Optimal + 1 Designs	Optimal + 2 Designs	Optimal + 3 Designs
Number of Existing Nodes for Which Designs Are Possible (Note 1)	110	106	110	94
Least Number of N+2 Nodes	1	2	3	4
Greatest Number of N+2 Nodes	6	7	8	9
Average Number of N+2 Nodes per Design	3.76	4.85	5.76	7.36
Percentage Increase Relative to Optimal	-	29%	53%	96%
Least New Fibre Metres	0	38	66	108
Greatest New Fibre Metres	3478	4357	4866	6301
Average New Fibre Metres	833	1,168	1,547	1,909
Percentage Increase Relative to Optimal	-	38%	86%	111%

Note 1: one existing node (Node CG949A) was determined to be a test node with no downstream active devices, so was discounted in counting valid designs and calculating averages per existing node.

With regard to time-savings, the automated design engine required about one hour of time to process all 552 technically valid N+2 designs across the 111 existing node areas and deliver the design data files for the optimal preliminary design for each existing node. By comparison, operator's personnel produced a single conceptual (i.e., significantly less detailed) design in about one hour.

4.2.2. N+2 Pilot Deployment #2

This pilot deployment was undertaken in 2020 with an operator that was considering a N+2 architecture as its general standard for all of its network upgrade work in the coming few years recognizing that, in certain cases, a N+0 architecture may be required and, in other cases, N+3 (or greater than three) may be entirely appropriate. For the purposes of the pilot deployment, a N+2 network architecture was specified. The automated design and optimization platform was deployed across approximately 150 existing node areas in three different markets served by the operator.

As with the previous N+2 pilot deployment, new nodes were to be placed only at locations of existing active devices, and the RF performance of the coaxial network was assumed to be in compliance with the operator's specifications both before and after the placement of new N+2 nodes.

Similarly, the automated design engine produced practically every possible technically valid N+2 preliminary design for each of the 150 node areas and the optimization function ranked the designs from lowest to highest capital cost estimate.

The findings of this pilot deployment in terms of capital cost optimization and savings for both new nodes and fibre cabling were consistent with those of the previous N+2 pilot deployment and were easily observed by the operator in reviewing the detailed bills-of-materials produced for each of the technically valid N+2 designs for each existing node area.

In this pilot deployment, a simple schematic view of each N+2 design for each existing node area was produced as shown in Figure 3. The availability of this view to both the operator's network engineering personnel and to the author's colleagues led, very satisfyingly, to the articulation of a number of network analysis and design techniques used intuitively by the network engineers. These techniques were then incorporated into the automated design and optimization platform. The result was the production of increasingly efficient optimal designs.

As shown in Figure 3, the optimal N+2 design comprises:

- Elimination of the original HFC node;
- Turning around of several of the existing amplifiers;
- Back-feeding of other existing amplifiers, and:
- The placement of five new N+2 nodes.

All of the non-optimal N+2 designs were also available in schematic view and were selectable using a drop-down menu in the upper left corner of the viewing window.

A complete bill-of-materials for each N+2 design was similarly available to the operator and served to allow evaluation and confirmation that, in fact, the optimal design had been produced by the automated design and optimization platform.

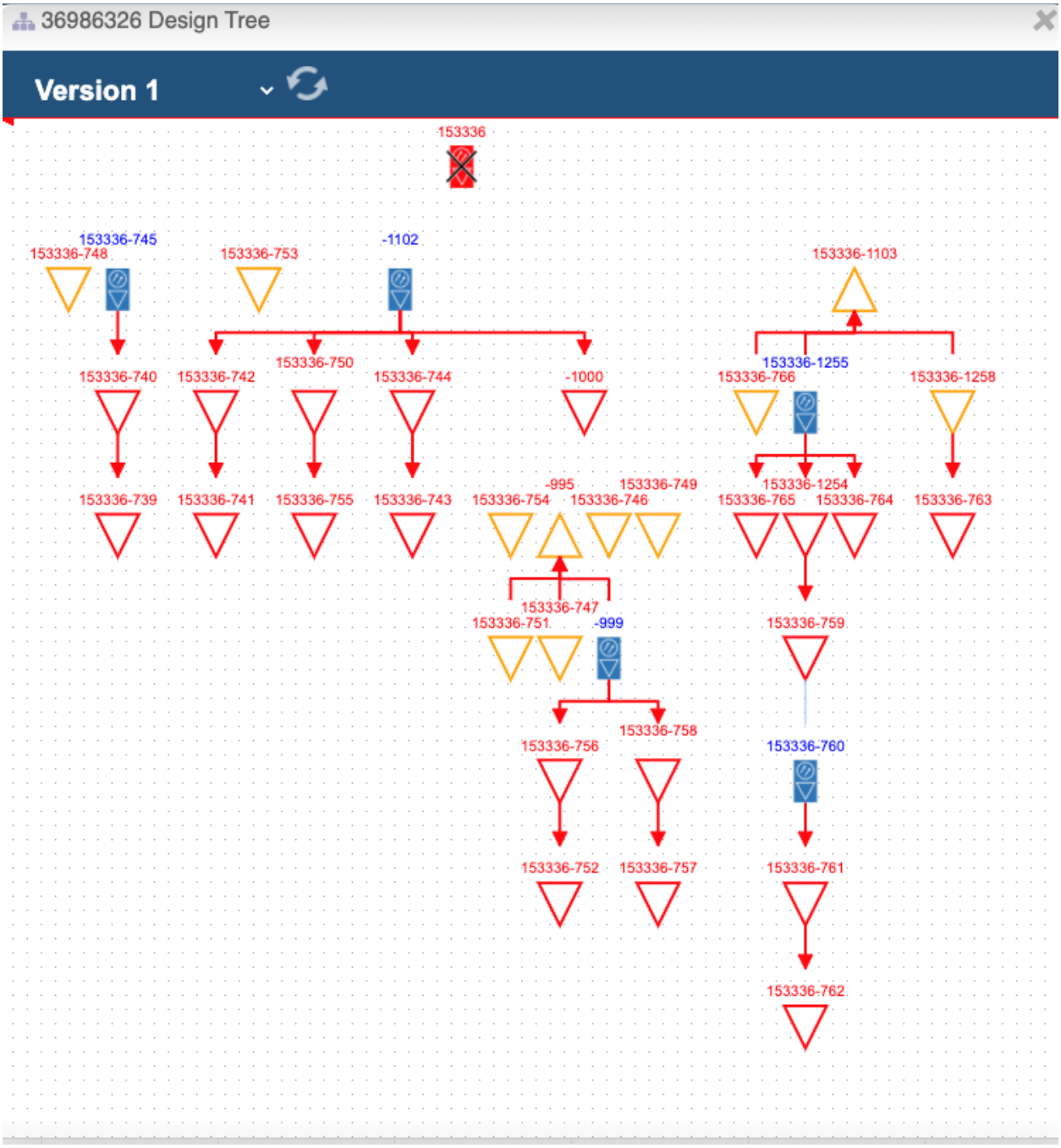

Figure 3 - Schematic View of Optimal N+2 Design

5. Conclusions

The results of the pilot deployments discussed in this paper indicate that cable operators can realize critically required operational improvements in their network strategy and network planning/engineering functions through the application of an automated design and optimization platform. These critical improvements include:

- Transformational time-savings in the strategic planning and preliminary design functions by reducing the preliminary design time to a matter of days or weeks from several months for a major network upgrade program;
- Significant capital cost savings relative to the traditional manual design methodology by taking advantage of the fact that the automated design and optimization platform will consistently deliver the lowest capital cost, technically compliant preliminary designs;
- Improved compliance with corporate engineering standards and practices across the operator's footprint by virtue of incorporating same into the automated design engine as design rules;
- Improved procurement forecasting and cost management through having detailed bills-of-materials available at the time strategic decisions are made, as opposed to months later when sufficiently detailed designs and bills-of-materials would otherwise become available;
- Reduced time and error in subsequent production of detailed network designs by importing preliminary design data files directly into the operator's engineering/GIS database, thus giving network engineers and drafting personnel an advantageous starting point from which to carry out their work.

Above all, the application of the automated design and optimization platform to the design of the access network offers the opportunity to relieve highly skilled network planners and engineers of the many tedious and time-consuming tasks they currently contend with and, instead, allow these valuable professionals to better respond to the demand for input to technology strategy decision-making and then for deployment of the access network itself.

Given the current environment of rapid technological advancement in, and increasing customer demand upon, the access network, it is expected that operators will only benefit by improving the effectiveness of their planning and engineering personnel through the use of the automated design and optimization platform.

6. Abbreviations and Definitions

6.1. Abbreviations

5G	fifth generation of cellular radio network technology
10G	branding adopted by cable operators for the evolution of cable networks from current data transmission capability to, ultimately, 10 gigabits/second in both the upstream and downstream directions
HFC	hybrid fibre/coax (hybrid fiber/coax)
ISBE	International Society of Broadband Experts
N+0	optical node having zero active devices in any one leg of the downstream RF coaxial network

N+2	optical node having a maximum of two active devices in cascade in any one leg of the downstream RF coaxial network
N+3	optical node having a maximum of three active devices in cascade in any one leg of the downstream RF coaxial network
SCTE	Society of Cable Telecommunications Engineers

7. Bibliography and References

Roaring Into The '20s With 10G; Howald, Dr. Robert; 2020 SCTE Tec-Expo Proceedings

Optimizing Node+0 Outside Plant Design for Cost and Energy Efficiency Using Artificial Intelligence; Ian Oliver; 2019 SCTE-ISBE Journal of Energy Management

Predicting the Number of Remote PHY Devices in a Hybrid Fiber/Coax Node+0 Deployment

A Technical Paper prepared for SCTE•ISBE by

Dr. Franklin M. Lartey, Director of Technology, Cox Communications, SCTE•ISBE Member
6305-B Peachtree Dunwoody Rd
Atlanta, GA 30328
Franklin.Lartey@cox.com / Franklin@Lartey.net
(404) 387-1866

Table of Contents

List of Figures

List of Tables

1. Abstract

In their quest to provide multi-gigabit speeds over hybrid fiber/coax networks, broadband companies have created a new fiber deep architecture known as node-plus-zero-amplifiers or N+0. This architecture allows broadband companies to deploy fiber deeper into their networks and remove existing actives such as amplifiers and line extenders. Prior to this study, there existed no empirical model allowing one to predict the number of digital nodes or remote PHY devices (RPDs) needed in an N+0 deployment. This study applied the principles of uncertainty reduction theory (URT) to identify determinants of the volume of RPDs required in an N+0 deployment and thus contributed to knowledge by reducing uncertainty related to the factors that influence this number.

The study used a sample of 771 HFC nodes designed for an N+0 architecture. This sample was split into two subsets: a training set representing 80 percent of the sample and a validation set representing the remaining 20 percent. A multiple regression statistical model was created using the training set and cross-validated against the retained set, achieving an accuracy rate of 96 percent suggesting good generalizability of the model.

The created model showed that the main determinants of the number of RPDs required in an N+0 deployment are: (a) the plant mileage; (b) the number of amplifiers on the plant; and (c) the number of households serviceable by the plant. Some limitations of the model were identified, one being the node design to signal exhaustion as opposed to maximization of homes passed or any other design strategy.

The findings of this study have implications for researchers and practitioners. From a research standpoint, a replication study can be conducted for one seeking to identify additional factors contributing to the number of RPDs needed in an N+0 deployment. From a practitioner standpoint, identifying the number of RPDs to purchase can help supply chain management (SCM) in their negotiations and discussions with vendors and the calibration of their warehouses. Forecasting the number of RPDs is also valuable to finance departments for the creation of the budget for the short- and long-range plans.

Keywords: uncertainty reduction; broadband; predict; remote PHY; RPD; forecasting; fiber node; HFC

2. Introduction

Since the inception of cable television technology, the cable network architecture has continuously evolved. One such evolution is the transformation from the all-coaxial plant to a hybrid fiber/coax (HFC) plant allowing cable operators to provide additional services, serve more homes farther on the network, and face growing competition (Lartey, 2020; Miguelez, 2017). A recent transformation of the HFC plant is commonly known as node-plus-zero-amplifier, also called Node+0 or simply “N+0” (Loeffelholz, 2017). Many broadband companies are currently transforming their HFC plants from a legacy analog architecture to this new N+0 design using remote PHY device (RPD) modules that are installed in optical fiber nodes. The R-PHY nodes are connected to the headend or hub using digital fiber links, commonly 10 gigabit Ethernet. The use of the term RPD to denote the digital remote PHY node is supported by current literature (e.g. Salinger, 2014; Liu & Chapman, 2020; Wall, Cooper, & Job, 2019).

To achieve the goal of providing multi-gigabit Internet speeds with no active device on the HFC plant, each existing HFC node (legacy node) must be replaced with a number of digital RPD nodes, depending on the number of homes serviceable by the node (households passed or HHP) among others. Because the deployment of digital nodes to replace legacy analog nodes requires a substantial capital investment from

operators, related costs need to be budgeted years prior to the deployment to accommodate capital budgeting timelines.

In addition, the RPD is not readily available on the market because it is a specialized equipment deployed by few operators. For that reason, manufacturers produce them just-in-time based on existing demand. It is thus important for operators to properly forecast the number of RPDs to deploy, which would ease material forecasting to SCM. This would help reduce the lead-time to obtain equipment, enable on-time project execution, and avoid stranded capitals due to excess materials in the SCM warehouses. Knowing the planned material volumes would also help SCM negotiate prices with the vendor, thus contributing to cost reduction.

Unfortunately, there is currently no study or literature allowing engineers to predict the number of R-PHY nodes required for the conversion to an N+0 architecture using RPDs. The goal of this study is two-fold: (1) to find factors that determine the number of RPDs needed to convert a legacy analog HFC plant into an N+0 architecture, and (2) to find a model predicting the number of RPDs needed in an N+0 deployment based on empirical data from current and past N+0 designs and deployments.

3. Literature Review

3.1. Theoretical Foundation: The Uncertainty Reduction Theory

This study is underpinned by the uncertainty reduction theory, not in the sense of interaction between people (engineers), but that of interaction between people and things (engineers and fiber nodes). The URT advocates the need by people to reduce uncertainty about others through the acquisition of knowledge related to the latter. In the case of this study, there is currently no existing knowledge on factors that determine the number of RPD nodes required in an N+0 deployment. This study will help reduce such uncertainty through the analysis of existing designs and deployments.

Created by Berger and Calabrese (1975), uncertainty reduction theory seeks to explain the communication pattern between two strangers in quest of reducing uncertainty and building a relationship. Berger and Calabrese explain that the more information obtained on someone, the more uncertainty about the person is reduced.

In a different study, Berger and Bradac (1982) posit that the greater the possibilities or options for a sought information, the greater the level of uncertainty. In identifying the drivers of the number of RPD nodes to deploy in an N+0 architecture, there exist many different options and possibilities, hence a higher level of uncertainty. This uncertainty is reduced by engineers who consider only a limited number of options such as the number of homes serviceable by the node, the plant mileage, the type of serviceable homes including single family units (SFU) and multi-dwelling units (MDUs), the type of plant (aerial or underground), and the plant density calculated as total plant mileage divided by total homes serviceable. By doing this, the engineers are the ones interacting with the nodes in a one-way information seeking relationship which is different from the social relationship suggested by the URT.

A further elaboration of this theory by Berger (1979) suggests three uncertainty reduction strategies, namely active, passive, and interactive. In the active strategy, one person seeks information from the other through verbal and nonverbal messages to which the other person reacts. The passive strategy consists of simply analyzing the other person's behavior or using any other unobstructed mean. In the interactive or third strategy, both people participate in bidirectional information exchange.

This study used the passive strategy of the uncertainty reduction theory to identify factors that determine the number of nodes to deploy in a fiber-deep N+0 architecture. This would help reduce uncertainty on the number of nodes and increase predictability thus helping SCM in their negotiations and discussions with vendors and the calibration of the warehouses for the turnover of quantities to deploy.

3.2. Architecture of an N+0 Node

The HFC network is used for last mile delivery of broadband services such as Internet, video, and voice to end customers. Information is served from the headend to the customer using the HFC plant (Lartey, 2017). After leaving the headend, the information is carried through fiber to the HFC node as shown in Figure 1. In the node, the signal received in the form of light is converted into an electric signal and transmitted using the appropriate frequency to the end customer through coaxial cables. The signal is amplified using amplifiers and line extenders to serve customers located farther on the network. Figure 1 presents an example of a node service area to help understand its conversion to a Node+0 amplifier architecture.

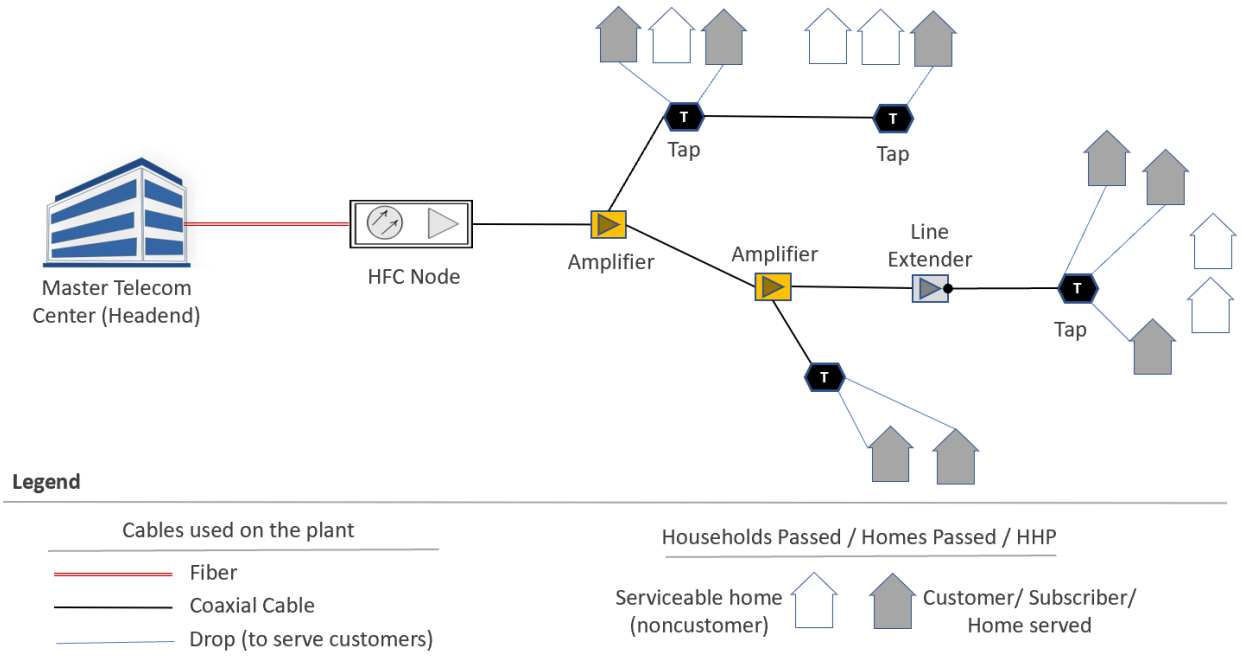

Figure 1 - Outside plant view of a legacy HFC Node prior to conversion to N+0

Figure 2 shows the same access network as in Figure 1 but this time, the plant has been converted to a Node+0 architecture. In this configuration, all amplifiers and line extenders were removed from the plant and fiber was deployed deeper in the plant, thus the qualification of "fiber deep" used by some researchers and practicians (Lartey, McGinn, & Diponzio, 2016). At this point, the only actives on the plant requiring powering are the RPD nodes; everything else is passive. In the illustrated example, one legacy analog node was converted into two digital RPD nodes to serve current and future customers in the footprint.

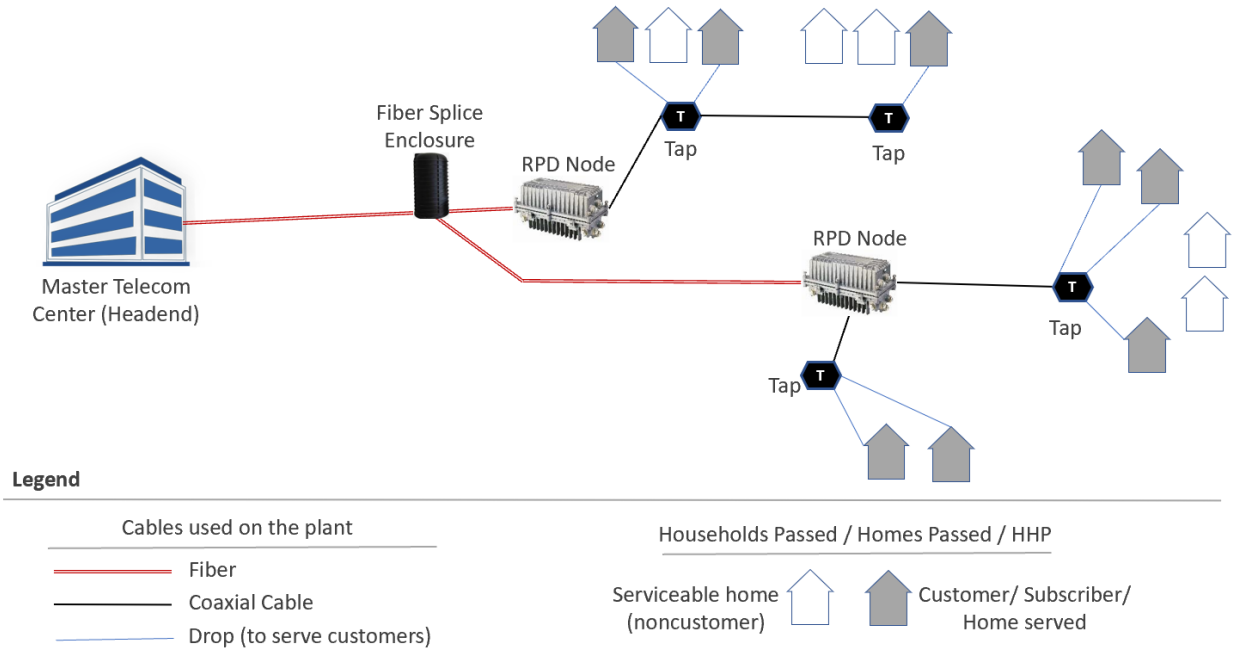

Figure 2 - OSP view of an HFC node converted to N+0 architecture with amplifiers and line extenders removed

As presented earlier, the main issue to address is how to plan and predict the number of RPD nodes required in an N+0 deployment. This is necessary because different nodes have different characteristics such as number of homes passed, coaxial plant, etc. Engineers are currently using some preliminary practices to predict the number of RPDs needed and some questions remain unanswered.

3.3. Current Practices

In conducting this research, two RPD node predicting formulas were identified. The first was based on an engineering observation that an RPD serves about 50 homes passed on average. The second was based on a more diligent analysis from the engineering team. It found that the number of RPDs required in an N+0 deployment depends on the total mileage and density of the node. The density in this case is the number of homes passed per mile. This engineering model suggested that the total number of nodes needed is 2.4 per existing coaxial plant mile if the density is less than 100 homes per mile. For nodes with densities greater or equal to 100 homes per mile, the number of nodes required to convert a legacy node into an RPD Node+0 configuration is one for every 100 homes passed (HHP). The two models were still experimental and are summarized as follows:

$$Y = roundup\ (HHP / 50) \qquad \text{(model 1)}$$

$$\begin{cases} If\ HHP/Mileage < 100,\ Y = roundup\ (mileage / 2.4) \\ If\ HHP/Mileage \geq 100,\ Y = roundup\ (HHP/100) \end{cases} \qquad \text{(model 2)}$$

In these models, Y is the number of nodes predicted for the conversion of an analog node into a passive N+0 architecture with digital RPD nodes. HHP is the number of homes serviceable on the HFC plant, also

referred to as households-past, homes past, or homes serviceable. HHP/Mileage represents the node density or number of homes passed per mile of coaxial plant.

4. Data Analysis and Results

4.1. Research Questions

In seeking the factors that determine the number of RPDs to deploy in an N+0 architecture, this study looked at the current practices and asked the research questions that follow.

RQ1: Does the number of households passed contribute to the number of RPDs required in a Node+0 deployment? If so, what is its contribution?

RQ2: Does the plant mileage contribute to the number of RPDs required in a Node+0 deployment? If so, what is its contribution?

RQ3: Does any other node factors such as the number of amplifiers contribute to the number of RPDs required in a Node+0 deployment? If so, what is its contribution?

RQ4: Does any combination of the identified factors contribute to the number of RPDs required in a Node+0 deployment?

For each of these research questions, a hypothesis and a null hypothesis were formulated. These are presented in what follows with H0x representing the null hypothesis for question x and HAx representing the alternate hypothesis for question x.

H01: The number of households passed does not contribute to the number of RPDs required in a Node+0 deployment

HA1: The number of households passed contributes to the number of RPDs required in a Node+0 deployment

H02: The plant mileage does not contribute to the number of RPDs required in a Node+0 deployment

HA2: The plant mileage contributes to the number of RPDs required in a Node+0 deployment

H03: The number of amplifiers does not contribute to the number of RPDs required in a Node+0 deployment

HA3: The number of amplifiers contributes to the number of RPDs required in a Node+0 deployment

H04: Combinations of the proposed factors do not contribute to the number of RPDs required in a Node+0 deployment

HA4: Combinations of the proposed factors contribute to the number of RPDs required in a Node+0 deployment

4.2. Sample Size, Missing Values, and Power Analysis

This quantitative cross-sectional research covered five states in the United States of America, namely Arizona, California, Nevada, Oklahoma, and Virginia, all served by the same broadband telecommunication company. The sample of the study consisted of all HFC nodes designed for a Node+0 deployment with RPDs. The initial sample size included 771 HFC nodes designed for N+0. Of these, 22 cases had missing values for AMPS and were removed from the dataset, leaving the study with 749 cases.

To allow for future cross-validation of the results, the dataset was split into two random samples using the function Data>Select Cases>Random Sample of Cases>80% in the Statistical Package for Social Sciences (SPSS) created by IBM. The study used the split sample of 80% (training data) for the creation of the regression model and 20% for the cross-validation of the model as recommended by Tabachnick and Fidell (2013). The final datasets included 614 cases for the training dataset or 80% split, and 135 cases for the test or validation dataset representing the 20% split. It is worth noting that SPSS does not do an exact 80/20 split, but randomly approximates the numbers. The sample size used for the creation of the regression model was thus made of 614 cases.

To ascertain the effect size of this sample, a post hoc power analysis was conducted using GPower 3, a statistical power analysis tool promoted by Faul, Erdfelder, Lang, and Buchner (2007) and previously used by Lartey, Hargiss, and Howard, (2015). The sample size of 614 was used for the power analysis along with three predictor variables as a baseline for the power equation. For reference, the following effect sizes were recommended by Cohen (1977): small ($f^2 = .02$), medium ($f^2 = .15$), and large ($f^2 = .35$). All three suggested effect sizes were used in this application with an alpha level of $p = .05$.

The post hoc analysis showed that the statistical power for this study was .84 for the detection of a small effect, but the power was a perfect 1.00 for the detection of moderate and large effect sizes. According to Cohen (1992), adequate power is obtained for values above .80. As such, there was more than adequate statistical power at all effect size levels.

4.3. Assumptions of Multiple Regression

In the quest to predict the number of remote PHY devices required for a Node+0 deployment, one dependent variable (DV) was identified and named RPD. It represents the number of remote PHY devices to deploy in an HFC node for the new N+0 topology. This variable is a scale measurement, resulting from the new design for the topology. In addition to the dependent variable, three independent variables (IV) were also identified and used namely MILEAGE, HHP, and AMPS. All three were continuous variable of scale measurement level in SPSS.

MILEAGE is the total coaxial plant mileage starting from the legacy node to the ends-of-line locations. This does not include drop cables that go from the tap to the home to serve the subscribers.

HHP represents the total number of households passed by the coaxial plant in the legacy node. This includes single family units, MDUs, business customers, and vacant lots. The units passed by the plant are not necessarily served but can all be served by the legacy node.

AMPS is the number of active components on the coaxial feeder of the legacy node. There are generally two main types of actives on the HFC plant: the amplifiers (AMP) with many outputs that amplify the input signal after it has travelled a certain distance, and the line extenders (LEs) that are also a type of amplifier with one output used to extend the network's reach to serve a remote location.

With the confirmation of the scale measurement level of all variables (DV and IV), the assumptions of multiple regression where tested. As presented by Tabachnick and Fidell (2013), these assumptions include: (1) univariate outliers or the absence of outliers among the IVs and the DV; (2) absence of multicollinearity and singularity; (3) multivariate outliers or absence of outliers in the solution; (4) ratio of cases to independent variables; and (5) normality, linearity, homoscedasticity of residuals, and independence of errors.

4.3.1. Univariate outliers

The number of cases used for the statistical regression analysis was 614 after removing 22 missing cases from the initial 771 and splitting the remaining dataset for future cross-validation. To identify univariate outliers, a descriptive statistic of all variables was executed in SPSS saving the standardized z-score values as variables. A subsequent descriptive statistic of the newly created z-score variables including only the minimum and maximum values showed the existence of z-scores above the recommended 2.68 suggesting the presence of univariate outliers. The problematic cases identified as outliers were eliminated from the dataset and the procedure was repeated until there was no further univariate outlier. In total, 69 univariate outliers were iteratively identified and removed, leaving the dataset with 579 cases for the analysis.

4.3.2. Multicollinearity and singularity

Multicollinearity occurs when a predictor or independent variable can be predicted from other predictors. In fact, independent variables need to be independent from each other with very low correlation among them. Collinearity diagnostics was computed using SPSS through the variance inflation factor (VIF) and tolerance. The output of the regression model showed the highest VIF at 4.7 and all collinearity tolerances calculated as *1 – SMC* (squared multiple correlations) scored above 0.2. Hence, all VIFs were well below the limit of 10 considered risky for collinearity and none of the tolerances approached zero. As a result, multicollinearity and singularity were not causes of concern in this study.

4.3.3. Multivariate outliers

The identification of multivariate outliers was done using the Mahalanobis distance of each case, then computing the probability that a value from the chi-square distribution with 3 degrees of freedom would be less than the Mahalanobis distance of the case as demonstrated by Tabachnick and Fidell (2013). To complete this, a new variable was computed using the Transform>Compute Variable option of SPSS. The equation specified for this variable was *1 – CDF.CHISQ(MAH_1,3)*, which is the same as using the SPSS function *SIG. CHISQ (MAH_1, 3)*, with 3 representing the degrees of freedom or number of independent variables (predictors) in each case. Any resulting variable less than the desirable alpha level of .05 indicated a multivariate outlier and was removed from the dataset, then a new Mahalanobis distance was computed. This process was repeated until there were no more multivariate outliers. Overall, 19 multivariate outliers were identified and removed from the dataset. This left the study with a total of 560 cases.

4.3.4. Ratio of cases to independent variables

After the removal of univariate outliers, there were 579 cases remaining. After further removal of 19 multivariate outlier cases, there were 560 cases left for conducting the regression analysis using three independent variables. This number was well over the minimum of 107 required. As explained by Tabachnick and Fidell (2013) and confirmed by Field (2013), for a medium size relation between the IVs

and the DV (α=.05, β=.20), the minimum number of cases required for testing individual predictors in a standard multiple regression is 104+n, where n is the number of independent variables.

4.3.5. Normality, linearity, homoscedasticity, and independence of residuals

A scatter plot was created using SPSS, with the standardized predicted values (ZPRED) on the x-axis and the standardized residual values (ZRESID) on the y-axis. The plot showed a rectangular pattern, and no point was outside the –3 to 3 range. In addition, the normal P-P plot and the regression standardized residual histogram confirmed that standardized residuals were normally distributed. Finally, the Durbin-Watson statistic showed a value of 2.09 confirming that residuals were not serially correlated from one observation to the next as explained by Field (2013). All the above suggested that the assumptions of normality, linearity, homoscedasticity, and independence of residuals were met, and the study could proceed with the elaboration of its results.

5. Results and Validation

5.1. Results

In this study, a standard multiple regression analysis was conducted to assess the ability to predict the outcome variable RPD using the independent variables HHP, MILEAGE, and AMPS representing respectively, households passed by the plant, plant mileage and amplifiers or actives in the plant. The analysis was performed with the statistical software package IBM SPSS version 24 using the functions Analyze>Descriptive statistics>Descriptives; Analyze>Descriptive statistics>Explore; and Analyze>Regression>Linear.

The analysis of variance (ANOVA) for the final model as shown in Table 1 confirmed that the overall regression model was significant $F(3, 556) = 796.01$, $p<.001$. Anova tests if the R-Square is significantly greater than 0. The p-value shown on Table 1 being less than .05 suggests that the R-Square is significantly greater than zero. As such, the predictors can account for an acceptable amount of variance in predicting the number of RPDs.

Table 1 - Analysis of Variance for the final model

Model		Sum of Squares	df	Mean Square	F	Sig.
1[a]	Regression	5777.283	3	1925.761	796.011	.000[b]
	Residual	1345.110	556	2.419		
	Total	7122.393	559			

a. Dependent Variable: RPD
b. Predictors: (Constant), AMPS, HHP, MILEAGE

The summary result of the multiple regression analysis is shown in Table 2. The R-Square indicates that 81.1% of the variance in the dependent variable (RPD) is explained by the three independent variables AMPS, HHP, and MILEAGE.

Table 2 - Multiple Regression Model Summary

Model	R	R Square	Adjusted R Square	Std. Error of the Estimate	Change Statistics					
					R Square Change	F Change	df1	df2	Sig. F Change	Durbin-Watson
1[b]	.901[a]	.811	.810	1.555	.811	796.011	3	556	.000	2.099

a. Predictors: (Constant), AMPS, HHP, MILEAGE
b. Dependent Variable: RPD

The *p*-value of all three independent variables is less than .001 as depicted in Table 3 indicating that the variables have a statistically significant impact on the outcome variable. In addition, the 95% confidence interval of the independent variables do not include 0 between the lower bounds and upper bounds (see Table 3), confirming the significance of the variables because none of them can be zero.

Table 3 - Coefficients of the Regression Model

Model		Unstandardized Coefficients		Standardized Coefficients	t	Sig.	95.0% Confidence Interval for B		Collinearity Statistics	
		B	Std. Error	Beta			Lower Bound	Upper Bound	Tolerance	VIF
1	(Constant)	1.135	.163		6.956	.000	.814	1.455		
	HHP	.005	.000	.262	10.664	.000	.004	.005	.562	1.779
	MILEAGE	.606	.054	.386	11.183	.000	.500	.713	.285	3.504
	AMPS	.131	.014	.375	9.292	.000	.103	.159	.208	4.798

Dependent Variable: RPD

The final model $F(3, 556) = 796.01$, $p<.001$, (see Table 1) has an R^2 of .81 (see Table 3). Because the *p*-value of each of the three variables used was significant ($p < .05$), the null hypothesis was rejected, suggesting that there was enough evidence that AMPS, HHP, and MILEAGE contribute in the number of RPDs needed in the deployment of a Node+0 HFC architecture. Indeed, the adjusted R^2 value of .81 indicated that 81 percent of variability in the number of RPDs on the entire network (population) can be explained using the three independent variables (AMPS, HHP, and MILEAGE). Based on the findings of this study, the predictive model is represented as follows:

$$\mathbf{RPD = 1.135 + (.005 \times HHP) + (.606 \times MILEAGE) + (.131 \times AMPS)}$$

5.2. Cross-Validation

As previously discussed, the regression analysis was executed on a split dataset using the 80% split. The remaining 20% split contained 135 cases and was used to validate the resulting model using a split-sample validation technique. To achieve this goal, the filter previously splitting the dataset was reset to select all cases. Next, a new variable was created to contain all predicted values using the function Transform>Compute Variable. This variable was named PREDICTED and its value was set to be computed using the formula:

PREDICTED=1.135+(.005*HHP)+(.606*MILEAGE)+(.131*AMPS)

Another variable was created to group each of the two data subsets using the Transform>Compute Variable function. This new variable was named SAMPLE and initiated to the filter variable previously

generated by SPSS for the data split. Additionally, using the variable tab on the dataset, the values field of this variable was updated to reflect the following labels: 0="20% Sample"; 1="80% Sample". The data was then grouped using the function Data>Split File>Compare Group>Group Base on SAMPLE.

Finally, the validation was done through a correlation analysis using the SPSS function Analyze>Correlate>Bivariate and including the variables PREDICTED and RPD. The result of the correlation analysis between groups is shown in Table 4.

Table 4 - Cross-validation through group comparison

SAMPLE			PREDICTED	RPD
20% Sample	PREDICTED	Pearson Correlation	1	.880**
		Sig. (2-tailed)		.000
		N	135	135
	RPD	Pearson Correlation	.880**	1
		Sig. (2-tailed)	.000	
		N	135	142
80% Sample	PREDICTED	Pearson Correlation	1	.924**
		Sig. (2-tailed)		.000
		N	614	614
	RPD	Pearson Correlation	.924**	1
		Sig. (2-tailed)	.000	
		N	614	629
**. *Correlation is significant at the 0.01 level (2-tailed).*				

The output on Table 4 shows that using the formulated equation, the correlation coefficient for the 80% sample is .92 while that of the 20% sample is .88. The accuracy rate of the holdout sample is .92 – .88 = .04. It is equals to 4%, which is within 10% of the training sample. Such high accuracy is enough evidence to confirm the validity of the multiple regression model presented. With this validation, the model is deemed generalizable notwithstanding its limitations discussed further in this study.

5.3. Predictive Power and Alternate Models

With the validation of the final model, the pending question sought the strengths of other possible models based on partial combinations of the three predictors. To that effect, various sub-models were created as shown in the summary in Table 5.

As shown in Table 5, each line represents information on a specific model. Altogether, seven models were created. The first column on the table shows the model number. It is followed by the predictors used to create the model. The most important value for each model is its R-Square which represents the proportion of variance in the sample explained by the model.

Table 5 - Summary of all models based on combinations of the three predictors HHP, MILEAGE, and AMPS

Model	Predictors	R	R Square	Adjusted R Square	Std. Error of the Estimate	Durbin-Watson
1	HHP	.65	.42	.42	2.708	1.658
2	MILEAGE	.81	.65	.65	2.114	1.685
3	AMPS	.86	.75	.75	1.801	1.732
4	HHP+MILEAGE	.88	.77	.77	1.712	1.669
5	HHP+AMPS	.88	.77	.77	1.720	1.766
6	MILEAGE+AMPS	.88	.77	.77	1.706	1.694
7	HHP+MILEAGE+AMPS	.90	.81	.81	1.555	2.099

Dependent Variable: RPD

Table 6 - Coefficients of all models based on combinations of the three predictors HHP, MILEAGE, and AMPS

Model		Unstandardized Coefficients		Standardized Coefficients	t	Sig.	95.0% Confidence Interval for B		Collinearity Statistics	
		B	Std. Error	Beta			Lower Bound	Upper Bound	Tolerance	VIF
1	(Constant)	2.786	.259		10.773	.000	2.278	3.294		
	HHP	.011	.001	.652	20.516	.000	.010	.012	1.000	1.000
2	(Constant)	2.857	.170		16.845	.000	2.524	3.190		
	MILEAGE	1.273	.039	.806	32.479	.000	1.196	1.350	1.000	1.000
3	(Constant)	2.434	.148		16.484	.000	2.144	2.724		
	AMPS	.302	.007	.864	40.461	.000	.287	.317	1.000	1.000
4	(Constant)	.984	.175		5.629	.000	.640	1.327		
	HHP	.007	.000	.383	17.326	.000	.006	.007	.827	1.209
	MILEAGE	.022	.035	.646	29.263	.000	.953	1.090	.827	1.209
5	(Constant)	1.715	.171		10.029	.000	1.380	2.051		
	HHP	.003	.000	.196	7.420	.000	.003	.004	.597	1.675
	AMPS	.258	.009	.739	28.035	.000	.240	.277	.597	1.675
6	(Constant)	2.175	.143		15.164	.000	1.893	2.457		
	MILEAGE	.466	.058	.297	8.088	.000	.353	.580	.303	3.299
	AMPS	.215	.013	.616	16.774	.000	.190	.240	.303	3.299
7	(Constant)	1.135	.163		6.956	.000	.814	1.455		
	HHP	.005	.000	.262	10.664	.000	.004	.005	.562	1.779
	MILEAGE	.606	.054	.386	11.183	.000	.500	.713	.285	3.504
	AMPS	.131	.014	.375	9.292	.000	.103	.159	.208	4.798

Dependent Variable: RPD

Table 6 can be used to express all models derived from partial combinations of the predictors. It shows the unstandardized coefficients (B) to use to that effect. It was used to answer all research questions.

RQ1: Model 1 in Table 6 shows that the HHP is significant in predicting the number of RPDs needed to deploy an N+0 architecture. As such, the null hypothesis H01 was rejected and the alternate hypothesis HA1 retained.

RQ2: Model 2 in Table 6 shows that the mileage is significant in predicting the number of RPDs needed to deploy an N+0 architecture. As such, the null hypothesis H02 was rejected and the alternate hypothesis HA2 retained.

RQ3: Model 3 in Table 6 shows that the number of actives (amplifiers + line extenders) is another factor significant in predicting the number of RPDs needed to deploy an N+0 architecture. As such, the null hypothesis H03 was rejected and the alternate hypothesis HA3 retained.

RQ4: Models 4, 5, 6, and 7 in Table 6 show that every combination of HHP, MILEAGE, and AMPS was significant in predicting the number of RPDs needed to deploy an N+0 architecture. As such, the null hypothesis H04 was rejected and the alternate hypothesis HA4 retained.

The R-Square column in Table 5 (which is the same represented in Table 7) was used to identify the contribution of each model to the overall number of RPDs to deploy. The first model (model 1) in Table 5 was based on the households passed. Its R-Square suggested that 42% of the variance in the outcome (RPD) was accounted for by the HHP. The second model based on MILEAGE showed an R-Square of .65 suggesting that 65% of variance in the outcome was explained by the MILEAGE. The third model based on AMPS showed that 75% of variability in the outcome is explained by the AMPS alone.

Interestingly, any model based on the combination of two of the three predictors accounts for 77% of variability in the outcome (models 4, 5, and 6). Ultimately, model 7 was the final model based on all three predictors and presented earlier in this study. It accounted for 81% of the variability in the outcome variable RPD.

Based on the information in Table 6, all models were expressed by their regression equations. Table 7 shows this expression in the column labeled “Equations Expression”.

Table 7 - Regression equations of all models based on combinations of the three predictors

Model	Predictors	Equations Expression	R Square
1	HHP	**2.786 + (.011 * HHP)**	.42
2	MILEAGE	**2.857 + (1.273 * MILEAGE)**	.65
3	AMPS	**2.434 + (.302 * AMPS)**	.75
4	HHP+MILEAGE	**.984 + (.007 * HHP) + (1.022 * MILEAGE)**	.77
5	HHP+AMPS	**1.715 + (.003 * HHP) + (.258 * AMPS)**	.77
6	MILEAGE+AMPS	**2.175 + (.466 * MILEAGE) + (.215 * AMPS)**	.77
7	HHP+MILEAGE+AMPS	**1.135 + (.005 * HHP) + (.606 * MILEAGE) + (.131 * AMPS)**	.81

6. Discussions and Conclusion

This study filled a gap in existing knowledge in the broadband industry by identifying a model allowing to predict the number of remote PHY devices needed in the deployment of a node+zero amplifier architecture. In so doing, it identified the main drivers of RPD volume as being the amplifiers, the coaxial plant mileage, and the households passed (serviceable) by the plant. When only one of these factors is known for a node, the number of amplifiers is a better predictor of the number of RPDs needed, accounting for 75% of variability in the outcome. This is followed by the mileage (65% of the variability), and the homes passed (42% of the variability). Interestingly, if two factors are known, regardless of the combination, the model accounts for 77% of variability in the outcome. When all three factors are known, the model accounts for 81% of variability.

In seeking the factors that determine the number of RPDs needed to convert a legacy analog HFC plant into an N+0 architecture, a multiple regression model was created using 80 percent of the 714 cases gathered for the study. The remaining 20 percent of the data was used to validate the resulting model. The split-sample validation indicated a high level of accuracy allowing for the generalization of the model in similar situations notwithstanding some limitations.

While providing a positive outlook, this study has some limitations needing to be addressed. Indeed, it still needs to be replicated prior to generalization in a different environment. The node design principles need to be considered, because the study was done in an environment where the nodes were designed to RF signal exhaustion. Other types of design could produce different results. In addition, this study was done on N+0 deployments with RPDs. Its results should not be generalized in situations where the N+0 is being deployed on analog nodes. With the constant changes in the industry, the model will need to be validated with every new architecture or technology introduced on the network as it has the propensity of increasing or reducing the signal depletion distance, thus the number of RPDs needed.

Despite the aforementioned limitations, this study has implications for researchers and practitioners. From an academia standpoint, it offers an opportunity for a replication study to validate the findings in a different environment. It also offers an opportunity to identify additional factors that could contribute to the number of RPDs required in an N+0 deployment. From a practitioner standpoint, the study will help reduce uncertainty on the number of nodes to purchase and increase predictability thus helping SCM in their negotiations and discussions with vendors and the calibration of the warehouses for the turnover of quantities to deploy. In addition to SCM, identifying the number of RPDs is useful for the finance team when creating the budget for upcoming years. In that regard, finance can adjust the budget accordingly and create properly executable budget plans allowing to view long term financial impacts of N+0 deployments on the organization's bottom line.

7. Abbreviations

ANOVA	analysis of variance
DV	dependent variable
Gbps	gigabits per second
HFC	hybrid fiber/coax
HHP	households passed
ISBE	International Society of Broadband Experts

IV	independent variable
LE	line extender
MDU	multi-dwelling unit
N+0	node plus zero amplifier
RF	radio frequency
RPD	remote PHY device
SCM	supply chain management
SCTE	Society of Cable Telecommunications Engineers
SFU	single family unit
SMC	squared multiple correlations
SPSS	Statistical Package for the Social Sciences
URT	uncertainty reduction theory
VIF	variance inflation factor

8. Bibliography and References

Berger, C. R. (1979). Beyond initial interaction: Uncertainty, understanding, and the development of interpersonal relationships. In H. Giles & St. Clair (Eds.). *Language and Social Psychology* (pp. 122-143). Oxford: Blackwell.

Berger, C. R. & Bradac, J. J., (1982). *Language and social knowledge: Uncertainty in interpersonal relations*. London, England: Edward Arnold.

Berger, C. R. & Calabrese, R. J. (1975). Some explorations in initial interaction and beyond: Toward a developmental theory of interpersonal communication. *Human Communication Research, 1*, 99-112.

Cohen, J. (1977). *Statistical power analysis for the behavioral sciences* (Rev. ed.). Hillsdale, NJ, US: Lawrence Erlbaum Associates, Inc.

Cohen, J. (1992). *A power primer*. Psychological Bulletin, 112(1), 155-159.

Faul, F., Erdfelder, E., Lang, A-G., & Buchner, A. (2007). G*Power 3: A flexible statistical power analysis program for the social, behavioral, and biomedical sciences. *Behavior Research Methods, 39*(2), 175-191.

Field, A. (2013). *Discovering statistics using IBM SPSS statistics* (4th ed.). Thousand Oaks, California, United States of America: SAGE Publications.

Lartey, F. M. (2017). Proactive Network and Technical Facilities Monitoring Using Standardized Scorecards. Technical Paper Proceedings from 2017 Fall Technical Forum, Denver, CO October 17-20. *Society of Cable Telecommunications Engineers (SCTE) / International Society of Broadband Experts (ISBE), NCTA, Cablelabs*, 506-535.

Lartey, F. M. (2020). Predicting Product Uptake using Bass, Gompertz, and Logistic Diffusion Models: Application to a Broadband Product. *Journal of Business Administration Research 9*(2), 5-18. doi: https://doi.org/10.5430/jbar.v9n2p5

Lartey, F.M., Hargiss, K., & Howard, C. (2015). Antecedents of customer satisfaction affecting broadband loyalty: An implementation of SERVQUAL and NPS. *International Journal of Strategic Information Technology and Applications, 6*(1), 26-41. doi: 10.4018/IJSITA.2015010103

Lartey, F. M., McGinn, R., & Diponzio, N. (2016). Reducing the cost of fiber-to-the-home brownfield deployment through the implementation of core extraction on an HFC network. *Journal of Network Operations, 1*(2), 78-90.

Liu, T. & Chapman, J. T. (2020). Building the RPHY upstream scheduler with YANG. Technical Paper Proceedings from the Cable-Tec Expo 2020, Denver, CO October 13-16. *Society of Cable Telecommunications Engineers (SCTE) / International Society of Broadband Experts (ISBE), NCTA, Cablelabs*.

Loeffelholz, T. (2017). Fiber deep networks and the lessons learned from the field. *The Complete Technical Paper. Proceedings from 2017 Fall Technical Forum, SCTE-ISBE Cable-Tec Expo 2017*, 660-672. Denver, CO: SCTE-ISBE.

Miguelez, P. (2017). Moving towards the light: Migrating MSO FTTP networks to a distributed access architecture. *The Complete Technical Paper. Proceedings from 2017 Fall Technical Forum, SCTE-ISBE Cable-Tec Expo 2017*, 894-913. Denver, CO: SCTE-ISBE.

Salinger, J.D. (2014). Remote PHY: Why and how. Technical Paper Proceedings from 2014 SCTE Cable-Tec Expo, Denver, CO September 23-25. Society of Cable Telecommunications Engineers (SCTE) / Cablelabs.

Tabachnick, B. G., & Fidell, L. S. (2013). *Using multivariate statistics* (6th ed.). Upper Saddle River, NJ: Pearson.

Wall, B., Cooper, M. & Job, D. (2019). Practical considerations for full duplex deployments in N+X environments. *2019 Fall Technical Forum. Proceedings from 2019 SCTE Cable-Tec Expo*, New Orleans, LA September 30 - October 3. Society of Cable Telecommunications Engineers (SCTE) - Cablelabs.

Developments in Cable Network Frequency Response Characterization

A Technical Paper prepared for SCTE•ISBE by

Ron Hranac (Retired)
SCTE•ISBE Fellow Member
rhranac@aol.com

Table of Contents

List of Figures

1. Introduction

Cable network performance is dependent upon a variety of factors, including choice of architecture, design, construction and installation quality, and effective maintenance and troubleshooting practices. Ensuring that a cable network provides high-quality signals to subscribers means maintaining proper active device alignment and correct signal levels to minimize degradation by noise and distortions; eliminating (and preventing, to the extent possible) external interference such as ingress and direct pickup; and being proactive rather than reactive with respect to overall maintenance practices. One of the most effective ways to help achieve optimum network performance is by what has long been called system sweeping, a method of characterizing and maintaining ideal frequency response. In addition to keeping network frequency response in check, it is equally important to ensure that in-channel frequency response (ICFR) is optimum.

This document begins with the definition of frequency response, in particular from the perspective of the cable industry. An overview of frequency response characterization is provided, followed by a look at cable network and ICFR testing technology from the 1960s through the present. The current state of the art, discussed later, continues the trajectory of improvement reviewed in this document.

2. What is frequency response?

Frequency response is one of several metrics that can be used to determine the performance of a component, device, system, or network. The term frequency response is more accurately called complex frequency response, the latter a measure of magnitude- and phase-versus-frequency. According to Wikipedia,

> Frequency response is the quantitative measure of the output spectrum of a system or device in response to a stimulus and is used to characterize the dynamics of the system. It is a measure of magnitude and phase of the output as a function of frequency, in comparison to the input.

In cable industry vernacular, frequency response usually refers to just magnitude (amplitude)-versus-frequency and is a measure of the overall gain variation of a cable network or an individual channel as a function of frequency. Even from that perspective, frequency response is an important metric with which to characterize the health of the network and of individual channels.

A simple measure of magnitude-versus-frequency response can be obtained by applying a continuous wave (CW) carrier of a certain amplitude at the input to a device under test (DUT), as shown in Figure 1. The CW carrier's frequency is then varied or "swept" (while maintaining a constant amplitude) across a frequency range of interest for the DUT. The output of the DUT is measured and the results plotted graphically, similar to what is shown in Figure 2.

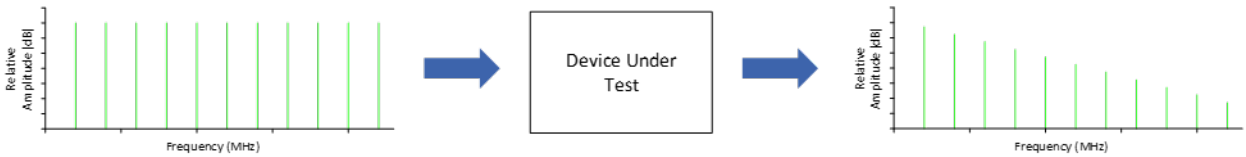

Figure 1 - Measuring the magnitude-versus-frequency response of a DUT using a constant-amplitude CW carrier whose frequency is varied continuously or stepped across a frequency range of interest.

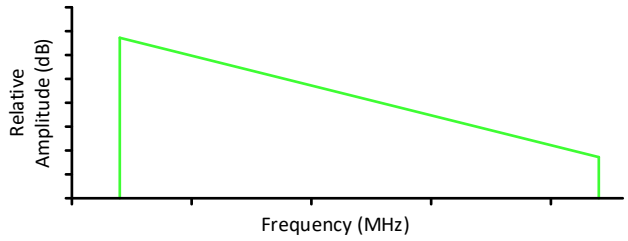

Figure 2 - Plotted magnitude-versus-frequency response of the DUT in Figure 1.

The frequency response of a cable network (or individual channels) can be characterized in several ways, using methods that include the following:

- true broadband sweep testing – usually high-level or low-level, either of which can produce a high-resolution frequency response characterization
- "connecting the dots" – that is, using the cable network's existing active signals as a reference to determine frequency response, with resolution limited to the spacing of the active signals
- injection of specialized signals called sweep points at specific frequencies (including in vacant spectrum) that are used as a frequency response reference – often in addition to the network's existing signals – to provide higher resolution than using just the network's existing active signals
- use of specialized baseband video test signals to determine the frequency response of headend modulators, and channel-specific sweep to determine the frequency response of headend processors
- observing a spectrum analyzer or similar spectrum display to get an approximation of the frequency response
- deriving from adaptive equalizer (or pre-equalizer) coefficients for single carrier quadrature amplitude modulation (SC-QAM) signals the in-channel frequency response and "splicing" those responses together to obtain an approximate response of the active passband

Each of these is discussed in more detail in subsequent sections of this document.

2.1. A closer look at frequency response testing

Cable operators for decades have characterized the frequency response of individual channels and the downstream and upstream spectrums in cable networks. Figure 3 shows examples of ICFR measurements, sometimes performed to ensure compliance with government regulations.

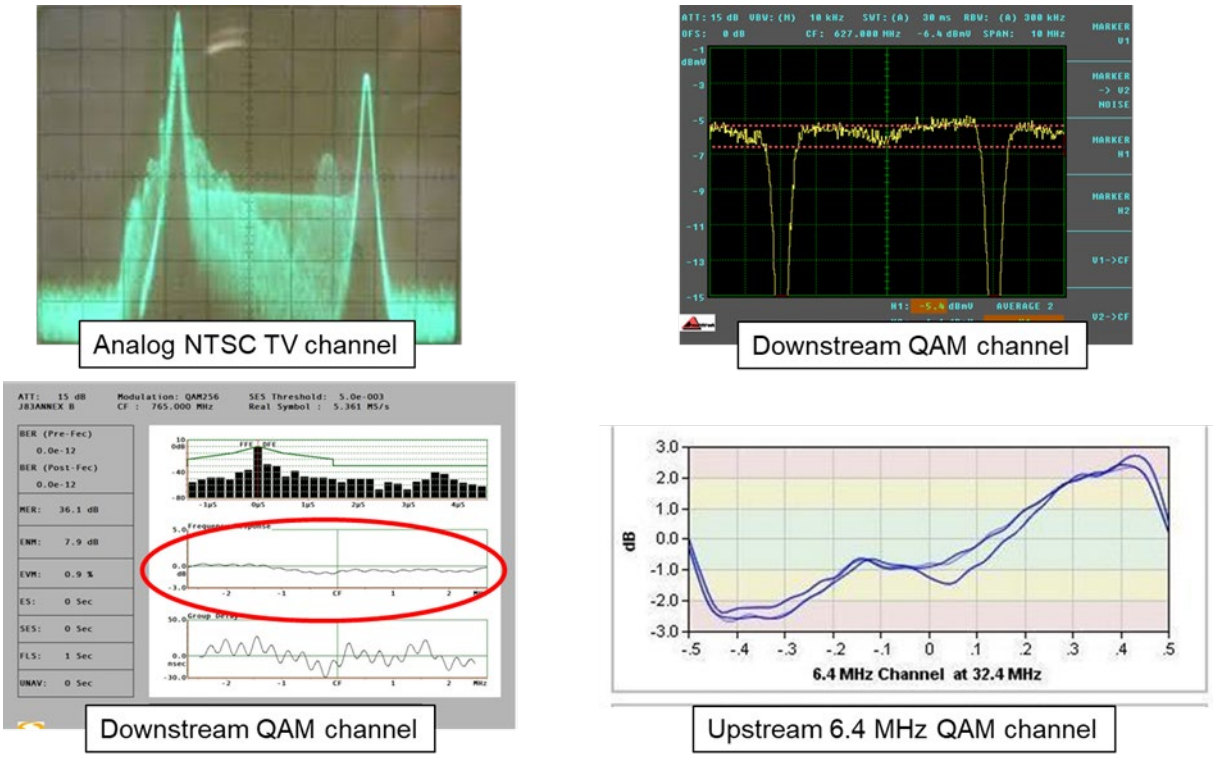

Figure 3 - In-channel frequency response measurement examples. Clockwise from upper left: use of SIN X/X baseband video test signal to characterize the in-channel response of an analog NTSC headend modulator; looking at the approximate in-channel response of an SC-QAM signal using a spectrum analyzer; adaptive pre-equalization-derived response of an upstream SC-QAM channel; adaptive equalization-derived response of a downstream SC-QAM channel (circled in red).

In-channel frequency response measurements for analog TV modulators were performed using specialized baseband video test signals such as multiburst, multipulse, NTC 7 combination, or SIN X/X, either full-field or as part of a vertical interval test signal (VITS). A field-rate baseband video sweep signal was used for measuring in-channel frequency response, too, but could not be part of VITS. Analog headend processors were commonly measured using a sweep signal injected at the antenna input. The in-channel frequency response of digital channels over their symbol rate bandwidth can be derived from adaptive equalizer or adaptive pre-equalizer coefficients. An approximation of a downstream SC-QAM signal's in-channel response can be observed on a spectrum analyzer display.

Characterizing frequency response of the entire operating spectrum in cable networks has commonly been done using some form of broadband sweep testing. One version of broadband sweep testing involves transmitting a sweep signal from the headend through the distribution network to characterize the downstream. That sweep signal comprises a test signal whose frequency varies ("sweeps") in a continuous or stepped manner across the bandwidth of the spectrum of interest. A receiver that is synchronized to the transmitter recovers the sweep signal during testing at various locations in the outside plant, allowing technicians to observe the frequency response. Sweep testing has been used to provide reference snapshots of the performance of the network at a given point in time, as well as for on-going or

periodic alignment, maintenance, and troubleshooting of amplifiers and other equipment in the outside plant. Figure 4 shows examples of cable network frequency response characterization.

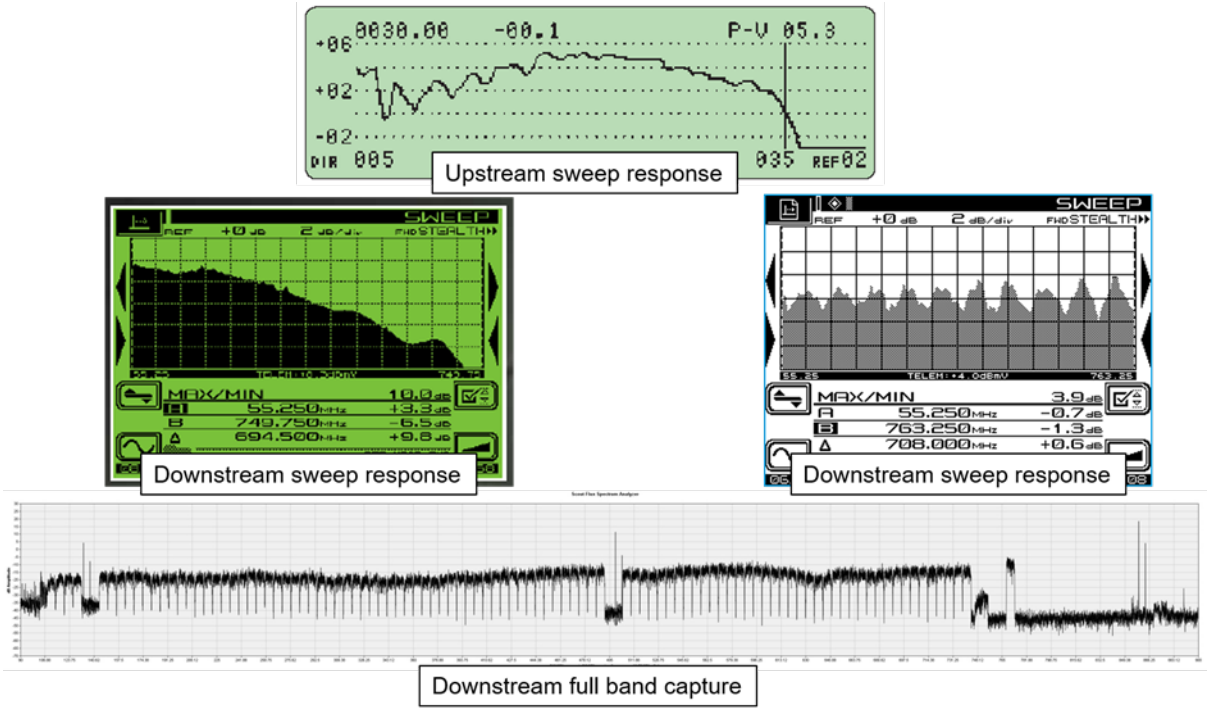

Figure 4 - Examples of cable network frequency response characterization. Clockwise from top: upstream frequency response; downstream frequency response showing presence of standing waves (amplitude ripple); full band capture display from a cable modem showing coarse response of the downstream spectrum; downstream frequency response showing excessive negative tilt.

3. Measuring frequency response

In most cases frequency response is measured or expressed in decibels (peak-to-valley or peak-to-peak) across a frequency range of interest. For example, the amplitude of a test signal or sweep signal at various frequency points is measured, with the results plotted on a graph or display of some sort. One can then determine the worst-case peak-to-valley amplitude-versus-frequency variation, as shown in Figure 5.

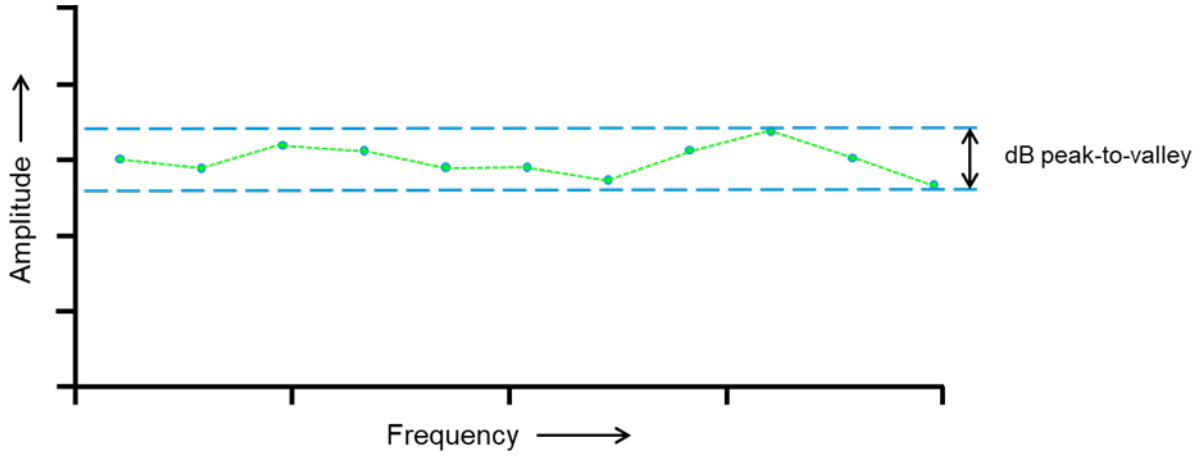

Figure 5 - Frequency response flatness.

Ideally, the plotted frequency response should be as flat as possible. But what amount of flatness is acceptable? First, it is important to understand that the concept of frequency response flatness can be complicated by the fact that frequency response tilt exists in cable networks, such as the positive tilt at the output of an amplifier. Fortunately, commercial sweep equipment has often included the ability to normalize tilt so the response trace appears horizontal on the sweep receiver display, making it easier to interpret the frequency response. See Figure 6.

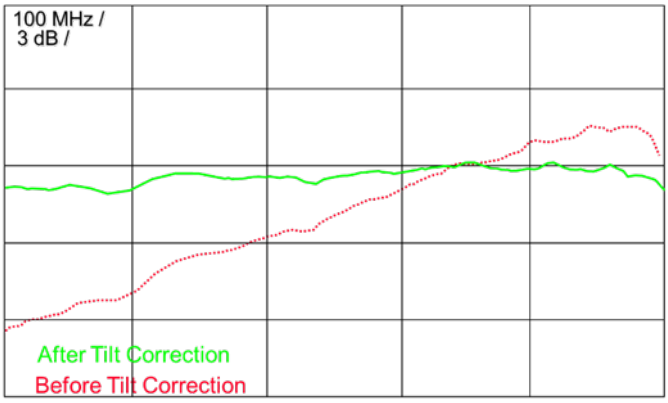

Figure 6 - Sweep receiver tilt compensation example (graphic from a Wavetek Wandel Goltermann training presentation; courtesy of Viavi Solutions).

In the past the following formula was widely used to determine the worst-case acceptable frequency response flatness in a cascade of amplifiers.

$$dB_{peak\text{-}to\text{-}valley} = (n/10) + x$$

where n is the number of amplifiers in cascade, and x is a sweep response factor usually provided by the amplifier manufacturer.

In all-coax tree-and-branch networks whose highest downstream frequency was below about 300 MHz, x was usually equal to 1. For example, the targeted end-of-line frequency response flatness for a 220 MHz 25 amplifier cascade was (25/10) + 1 = 3.5 dB peak-to-valley. As network RF bandwidth expanded beyond 300 MHz, x increased, too, to values such as 1.5 and 2. Over time – and as network bandwidth became even greater – the formula was no longer satisfactory.

4. Sweep or balance?

An amplifier alignment procedure variously known as balance, rough balance, or band edge balance has long been used for initial activation, adjustment, and quick checks of amplifiers in the outside plant. The procedure is straightforward: Measuring two RF signals – one at the low end of the downstream spectrum and the other at the high end of the downstream spectrum – a technician adjusts the amplifier to get its operation approximately correct with respect to input padding (attenuation) and equalization, and output RF levels and tilt. It's important to understand that balancing amplifiers does not replace sweep alignment. Looking at Figure 7, it's apparent that measuring the RF level of just the two signals cannot show what is happening across the entire spectrum.

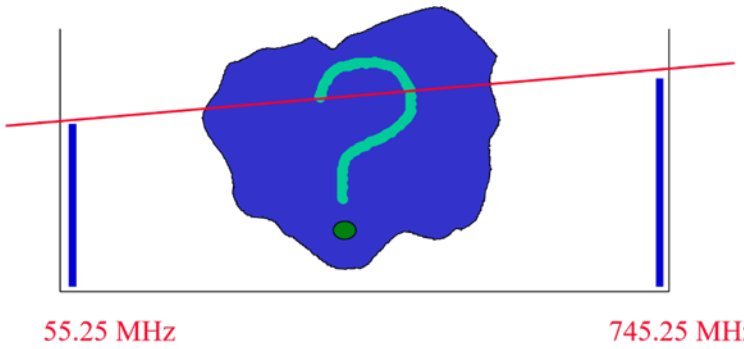

Figure 7 - Rough balancing is useful for ensuring that an amplifier is operating approximately correctly, but does not show the overall frequency response. There is no way to determine what is happening across the operating spectrum. Source: Wavetek Wandel Goltermann training material (courtesy of Viavi Solutions).

Sweep technology development over the years helped reduce manpower requirements for network sweep testing. In the early days of summation sweep, it wasn't unusual for two or three people to do the testing: one in the headend operating the sweep transmitter, and one or more in the field operating the detector, oscilloscope and other equipment. Integrated sweep equipment allowed downstream sweeping to become a largely one-person (per sweep receiver) operation. However, upstream sweep often needed two people: one operating the field unit (upstream sweep transmitter) and one monitoring the received sweep signal in the headend or another location. Here, too, technology improvements resulted in upstream sweeping becoming a one-person operation.

5. Early sweep testing

In the early days of sweep testing – through about the first half of the 1970s or so – the process was fairly crude and service disruptive. During the measurement, all downstream signals were turned off except for the automatic gain control (AGC) pilot and the sweep signal. At the time, broadband sweep testing was sometimes called summation sweep. The process was used to get a snapshot of the cable network's

frequency response, although it conceivably (and with some difficulty) could be used for outside plant maintenance/alignment. A broadband sweep generator was connected in the headend and configured to have start and stop frequencies slightly beyond the downstream operating frequency range (e.g., 45 MHz to 225 MHz for a network that carried 12 channels in the 54 MHz to 216 MHz spectrum).

As illustrated in Figure 8, the amplitude of the sweep signal was set 15 dB to 20 dB higher than normal analog visual carrier levels. A notch filter (trap) was installed at the output of the sweep transmitter and was tuned to the AGC pilot frequency to prevent sweep interference to AGC circuits in amplifiers. A wideband diode detector was connected to a suitable RF test point, and the output of the detector connected to an oscilloscope.

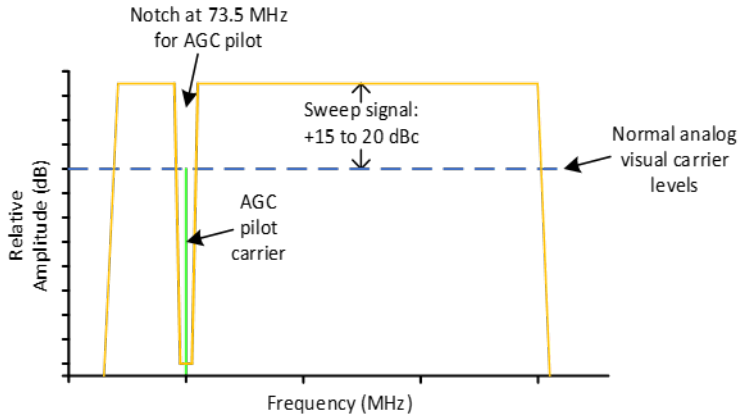

Figure 8 - Early summation sweep, showing a notch in the sweep signal at the AGC pilot carrier frequency. The yellowish solid line represents the sweep signal, and the dashed horizontal blue line the normal signal level of the network's analog visual carriers.

Figure 9 shows an example of the summation sweep test setup in the headend. After a reference was established, the sweep generator output and AGC pilot were connected to the headend's trunk feed.

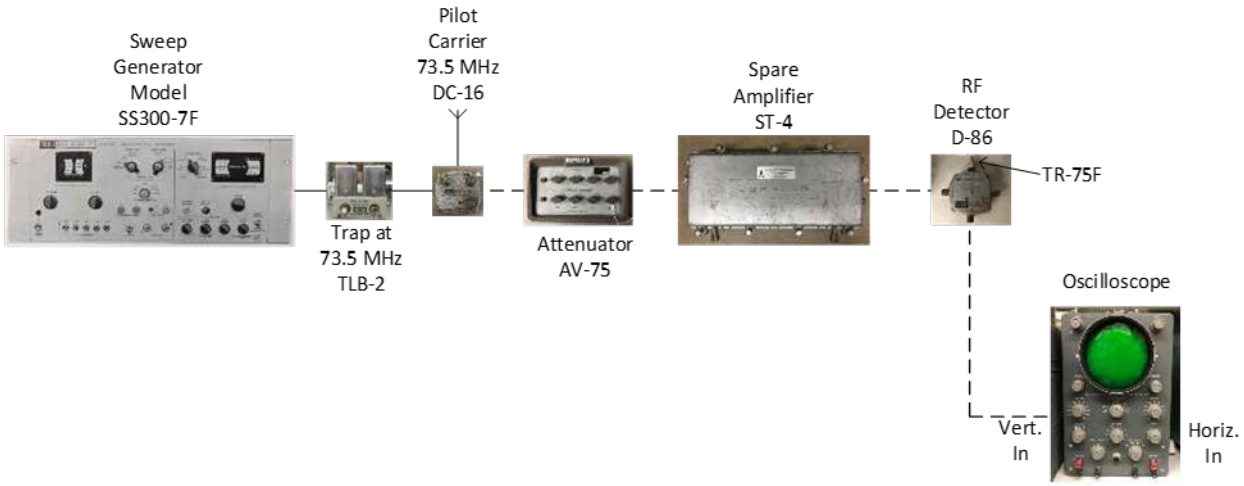

Note: The equipment connected via dotted lines is installed temporarily to set up a reference and will be removed during actual system sweep alignment.

Figure 9 - Summation sweep equipment block diagram showing the test setup in the headend. Adapted from a 1970s Jerrold Technical Seminar Manual; equipment photos taken at The Cable Center; used with permission of the Barco Library, The Cable Center.

During the sweep test, someone at the headend turned on the sweep generator, and the detector/oscilloscope combination in the field captured and displayed a trace that represented the swept frequency response of the network. Figure 10 shows an example of a block diagram of the equipment in the field.

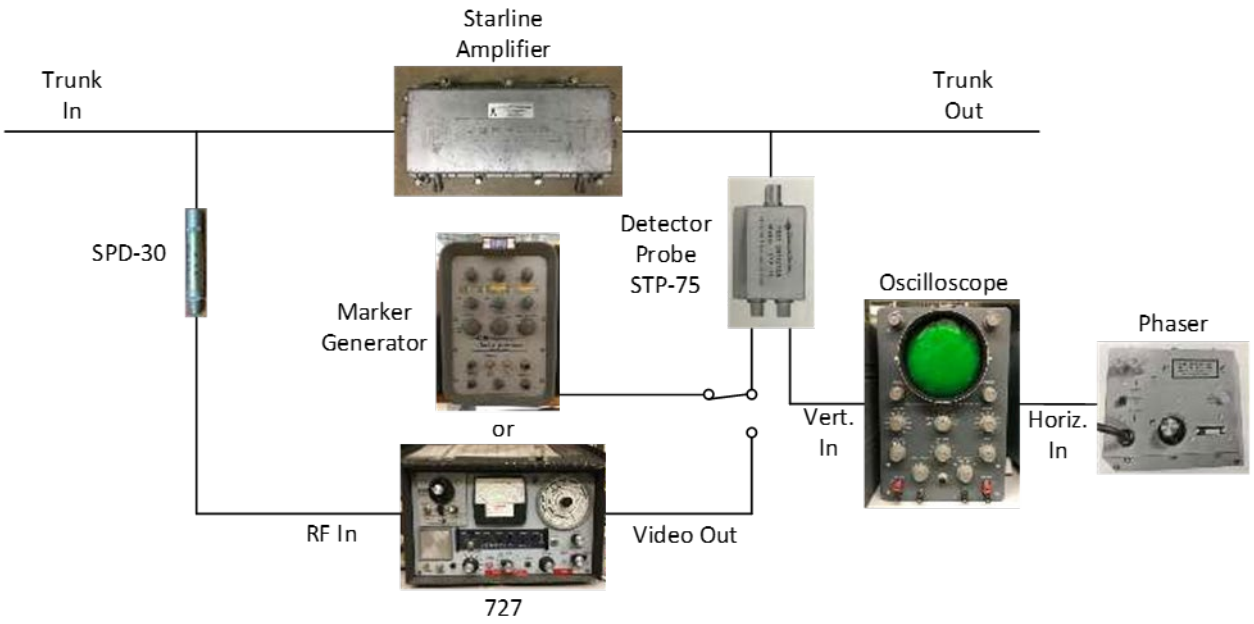

Note: Special application using 727 [field strength meter] as a variable marker generator

Figure 10 - Block diagram of summation sweep test setup in the field. Adapted from a 1970s Jerrold Technical Seminar Manual; equipment photos taken at The Cable Center (used with permission of the Barco Library, The Cable Center). SPD-30 photo courtesy of Bill Naivar.

(Note: Bench sweep setups have long been used for frequency response measurements and alignment of filters, headend processors, amplifiers, etc., but this equipment cannot easily be used to sweep a cable network. Examples of early sweep equipment – including bench sweep equipment – can be seen at The Cable Center in Denver, Colorado. See Figure 11.).

In the 1970s and ’80s test equipment manufacturers such as Jerrold/Texscan and Wavetek/Mid State combined several of the functions of the early summation sweep setups into integrated chassis: a sweep transmitter for the headend, and a sweep receiver (with built-in display) for the field. Both manufacturers’ products were high-level sweep systems and offered similar capabilities.

Figure 11 - Early bench sweep (photo used with permission of the Barco Library, The Cable Center).

6. High-level sweep

For instance, Wavetek's 1855/1865 broadband sweep signal was continuous and repetitive, and was received/displayed by a broadband sweep receiver calibrated in both frequency and amplitude. As such, techs could use the sweep receiver for routine amplifier alignment, troubleshooting frequency response problems such as suckouts, ripple, and so on. This was a high-level sweep (that is, the sweep signal operated at an amplitude higher than the visual carriers, typically 15 dB to 20 dB higher), so could potentially cause brief but perceptible interference to analog TV channels. Sometimes it could interfere with operation of scrambled channels. See Figure 12.

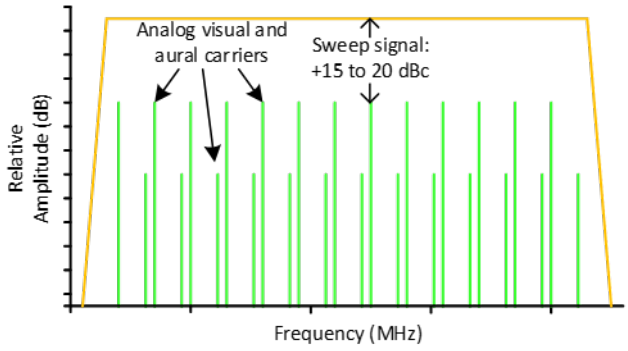

Figure 12 - Graphic showing amplitude of high-level sweep (yellowish trace) relative to visual and aural carriers (green).

Figure 13 - Wavetek 1855 sweep transmitter (photo taken at The Cable Center; used with permission of the Barco Library, The Cable Center).

Figure 14 - Wavetek 1865 sweep receiver (photo taken at The Cable Center; used with permission of the Barco Library, The Cable Center).

The headend sweep transmitter also generated a telemetry signal/pilot, placed in an unused part of the downstream spectrum such as just below Ch. 2. The telemetry signal was used to synchronize the sweep receiver with the sweep transmitter. Figure 13 and Figure 14 show examples of the Wavetek 1855 sweep transmitter and 1865 sweep receiver.

One of the interesting features that was developed for the 1855/1865 system was “normalization,” with which a response could be captured and stored at the first amplifier, then compared with subsequent responses at other amplifiers to show the change. No change in response meant the trace would be flat across the middle of the screen. The 1865 sweep receiver was reportedly the first field equipment made by Wavetek that incorporated microprocessors.

7. Low-level sweep

A company called Avantek (the same Avantek that manufactured semiconductors and other electronic components and devices) introduced a low-level broadband sweep product in the 1970s. Here, low-level means the continuously sweeping signal’s amplitude was set 30 dB lower than visual carrier levels, as illustrated in Figure 15.

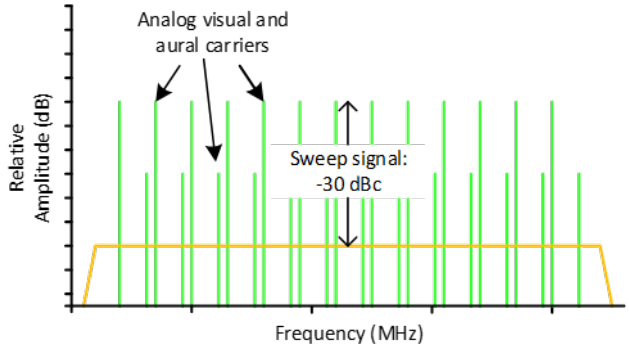

Figure 15 - Graphic showing amplitude of low-level sweep (yellowish trace) relative to analog visual and aural carrier levels (green).

Low level sweep reduced or eliminated interference to signals carried on the network. A sweep pilot was transmitted in the downstream just below Ch. 2 (around 50 MHz to 52 MHz), and was used for receiver synchronization. The Avantek receiver (Figure 16) was doubly useful in that in addition to a sweep receiver, the instrument incorporated a spectrum analyzer. The downside to the Avantek sweep system was that the sweep signal's low level could make it difficult to see the frequency response in really long trunk cascades because of the low carrier-to-noise ratio (CNR) near the ends-of-line. That said, a cable system where the author worked in the late '70s/early '80s used an Avantek low-level sweep system to maintain a 67-amplifier trunk cascade.

Figure 16 - Avantek sweep receiver, which included spectrum analyzer functionality (photo taken at The Cable Center; used with permission of the Barco Library, The Cable Center).

In later years, a company called Avantron acquired the rights to the Avantek low-level sweep technology. Avantron improved the Avantek line with a redesigned sweep transmitter (Figure 17) and a new spectrum analyzer (Figure 18) with better overall performance that also made the frequency response interpretation easier. In part because of the better performing spectrum analyzer, the price of the receiver was significantly higher than what was to come from other manufacturers. After Avantron was acquired by

Sunrise Telecom, and with the eventual integration of CaLan technology into the Sunrise family, the low-level sweep products were discontinued.

Figure 17 - Avantron AT2000G low-level sweep transmitter (courtesy of Bernie Cadieux).

Figure 18 - Avantron AT2000R spectrum analyzer with integrated low-level sweep receiver (courtesy of Bernie Cadieux).

8. Medium-level sweep

CaLan introduced what some have called a medium-level sweep system in the 1980s, whose design was said to be interference-free. Originally comprising the model 1777 transmitter and model 1776 receiver, frequency response characterization was done using measurement of injected signals called sweep points (set 10 dB to 15 dB below analog visual carrier levels) and existing signals carried in the network. Synchronization of sweep receivers in the field and the headend's sweep transmitter was accomplished via a downstream pilot carrier usually transmitted below Ch. 2, typically around 50 MHz or 51 MHz. While some other sweep systems relied upon the user programming the equipment where to transmit sweep points, the CaLan was unique in that guard bands were programmed around existing carriers where the sweep points should not be transmitted. Figure 19 shows a CaLan 1776 sweep receiver.

Figure 19 - CaLan model 1776 sweep receiver (photo from an old CaLan product brochure, courtesy of VeEX).

The CaLan 1777/1776 equipment evolved into the 3010 series (see Figure 20), and the product line was acquired by Hewlett Packard, Sunrise Telecom, and finally VeEX. The current product from VeEX is the 3010H+ downstream sweep transmitter/upstream sweep receiver, discussed later in this document.

Figure 20 - CaLan 3010 series sweep equipment (from an old Sunrise Telecom brochure, courtesy of VeEX).

9. Frequency response testing using existing network signals

Another approach to characterizing cable network frequency response is to use the network's existing signals as the measurement references. Viavi Solutions (formerly known as Wavetek, Wavetek Wandel Goltermann, Acterna, and JDSU) calls this method Sweepless Sweep™. The idea here is that the tech's field meter is used to measure RF signal levels of all downstream signals at a convenient amplifier test point (headend output, or node output in HFC plants). The field meter automatically normalizes those signal level measurements and stores them. Subsequent measurements are compared to the stored reference, and the difference produces a coarse indication of frequency response. The reference includes measurements of analog TV channel visual and aural carriers; later digital-compatible versions make multiple signal level measurements within each SC-QAM signal to further improve the resolution. Note:

Sweepless Sweep isn't true sweep; it's more like connect the dots. By itself it can't be used to characterize the frequency response of portions of the spectrum that do not carry signals. Figure 21 shows an example of a downstream frequency response measurement using a JDSU DSAM-6000 operating in Sweepless Sweep mode.

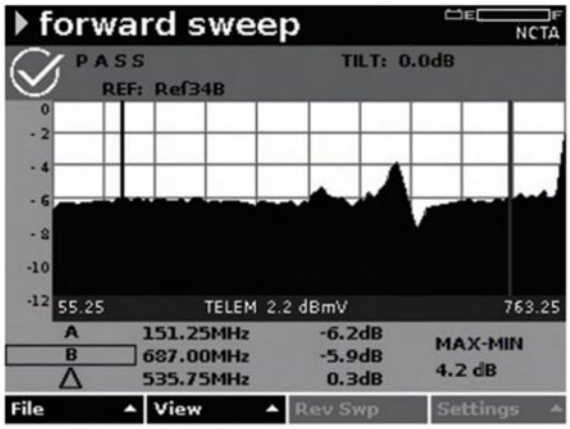

Figure 21 - Downstream Sweepless Sweep frequency response from JDSU DSAM-6000 (courtesy of Viavi Solutions).

To augment Sweepless Sweep and support frequency response testing of unused parts of the spectrum, a sweep transmitter (e.g., Wavetek Stealth 3ST, JDSU SDA-5500 transceiver, or the previously described CaLan equipment) in the headend could inject sweep points in vacant spectrum as well as in between adjacent channels. Those sweep points comprise an RF signal that very briefly appears at configured frequencies (see Figure 22). For instance, the sweep point signal turns on briefly at 52 MHz, turns off, then turns on at 74 MHz, turns off, turns on at 90 MHz, turns off, turns on at 100 MHz, and so on. All of this happens VERY fast. Downstream and upstream telemetry carriers allow communication and synchronization between the field units and headend unit. The sweep receiver measures both the injected sweep points and existing signals (analog TV, SC-QAM), and from that creates more "dots" to connect for the derived frequency response. All of this happens repetitively and more or less continuously, so that techs can align amplifiers, and do other troubleshooting/maintenance. One could argue that even with sweep points this isn't true broadband sweep (at least not continuous sweep), but can provide improved frequency response resolution compared to just Sweepless Sweep.

Note: The displayed resolution was limited by the screen size and number of pixels across the width of the screen. When sweeping 550 MHz or more, one may think the resolution is better than it really is. Even with a continuous sweep like the one from the previously discussed 1855 sweep transmitter, the displayed resolution was probably similar to that of a Sweepless Sweep in a fully loaded spectrum.

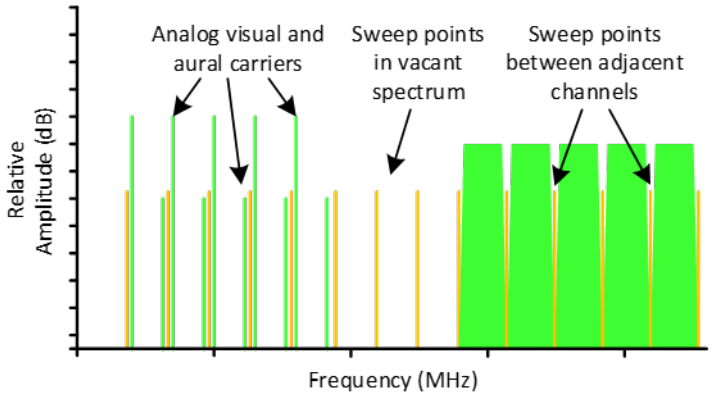

Figure 22 - Sweep points (yellowish lines) in vacant spectrum and in between adjacent channels.

Wavetek (later Wavetek Wandel Goltermann or WWG) had a sweep system known as Stealth, comprising the 3ST headend transmitter and 3SR field receiver (Figure 23). The Stealth 3ST and 3SR could operate in what was called Stealth mode, which used a combination of existing RF signals in the plant (analog TV signal visual and aural carriers plus digital signals) and injected sweep point signals for the frequency response reference, as shown previously in Figure 18. The Stealth's Sweepless Sweep mode used just the system's existing signals as the frequency response reference.

Figure 23 - Wavetek Stealth 3ST (rear) and 3SR (front). Source: Wavetek Wandel Goltermann training material (courtesy of of Viavi Solutions).

When set up for Stealth mode, the 3ST could be programmed to inject sweep point signals in between adjacent channels (typically about 1.1 MHz below each visual carrier), in between adjacent digital signals, and in unused spectrum. The sweep point nominal injection level was 14 dB to 16 dB below visual carrier levels. A downstream telemetry signal, often transmitted just below Ch. 2, synchronized the transmitter and receivers, and updated the receivers about changes to headend RF signal levels (which were also used as a frequency response reference). Figure 24 shows an example of a Stealth receiver's frequency response display.

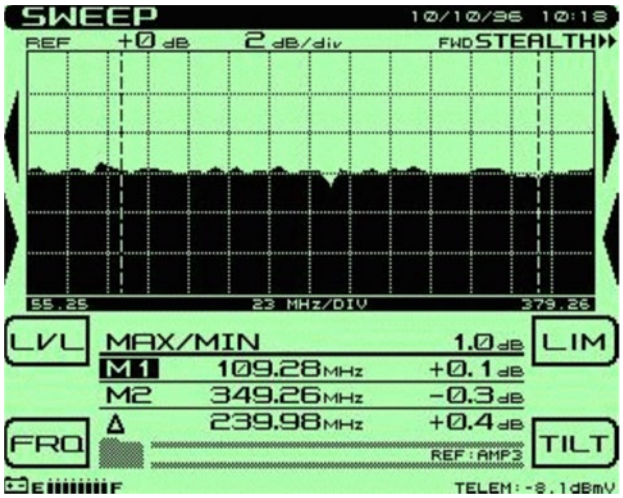

Figure 24 - Example screen shot from Stealth receiver. Image from Wavetek Wandel Goltermann training material (courtesy of Viavi Solutions).

The Stealth sweep system also supported upstream frequency response testing.

10. Another approach to interference-free testing

Figure 25 - Tektronix 2722 sweep receiver (photo from Tek Wiki, used with permission).

Tektronix had a novel approach to cable network frequency response testing with their model 2721 transmitter and 2722 receiver, products marketed in the late 1980s and early 1990s. Sometimes called a vertical interval sweep system or method, the transmitter injected a short duration sweep pulse in the channel (similar to a sweep point) coinciding with the vertical blanking interval of each TV channel's video, 11.5 microseconds after the midpoint of the first post-equalization pulse. The amplitude of the sweep signal was -6 dBc relative to visual carrier levels for non-gated measurements, and as low as -33 dBc for gated measurements. A telemetry carrier was transmitted in the downstream to receivers for synchronization. The technology was not compatible with digital signals and did not show the response of vacant parts of the spectrum. Figure 25 shows one of the model 2722 sweep receivers.

11. Return path frequency response testing

For upstream sweeping, a variety of methods have been used over the years. Some of the previously mentioned broadband sweep equipment could be used to produce an upstream display similar to what is shown in Figure 26. Other products rely upon sweep points, so the frequency response resolution is limited by the number of sweep points and how closely together they can be configured (the more active signals in the upstream, the fewer sweep points that can be used). The field unit generates the upstream sweep points, which are transmitted from the tech's location in the outside plant to the headend sweep controller. The headend controller connects the dots to get a coarse response, digitizes that information, and sends the data to the sweep receiver (recall that there are downstream and upstream telemetry

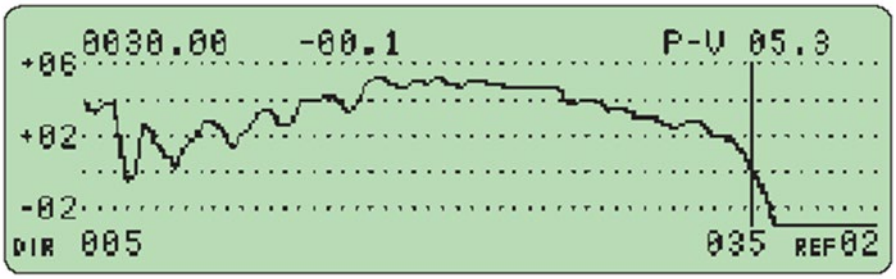

Figure 26 - Screen shot of upstream frequency response using CaLan sweep equipment (original CaLan graphic from Sunrise Telecom material; courtesy of VeEX).

carriers for communication and synchronization between the headend and field units). The sweep receiver out in the field then displays the upstream frequency response as "seen" by the headend controller, so the tech can see what the response looks like in the headend. This process is near real-time, although there is some latency between when the field unit transmits the sweep points and when the field unit displays what the headend controller "sees," but the latency is low enough that the tech can tweak a gain or tilt control in a reverse amplifier and a second or so later see the resulting response.

Figure 27 - Avantron BAS, the headend part of the company's two-carrier upstream alignment system. Photo from Bernie Cadieux.

12. Two-carrier method

Avantron offered a one-person operation dual-carrier reverse alignment system. A RAS/BAS-1 system allowed the RAS ("reverse alignment system," the field device) to inject two CW carriers from the field. The RAS was crystal-controlled, so the frequencies had to be chosen when the equipment was ordered –

for example, 5 MHz and 35 MHz. The RAS's upstream carriers were received at the headend by the BAS ("bi-directional alignment system," the upstream receiver – see Figure 27), the information processed, then digitized and sent back to the RAS unit by means of a downstream telemetry carrier. Upstream levels, as received by the BAS unit, were displayed by the RAS unit.

13. Multiple-carrier method

Trilithic (now part of Viavi) offered a one-person operation eight-carrier reverse alignment system, originally comprising the SST-9580 headend unit and SSR-9580 field unit. Operation was fairly straightforward: A technician in the field would connect an SSR-9580 (Figure 28) to a convenient test point, and the field unit would transmit up to eight pre-configured test carriers in the upstream back to the headend.

The SST-9580 in the headend received the upstream test carriers and "connected the dots" to show the coarse frequency response across the return spectrum. That information was digitized and sent downstream via a telemetry carrier to the SSR-9580, which displayed what the SST-9580 was "seeing" in the headend (example shown in Figure 29). The Trilithic 9580 equipment could also numerically display gain and tilt.

A handy troubleshooting feature of the Trilithic equipment was the ability for the SST-9580 to capture upstream spectrum information, digitize it, and send to the field unit so the field technician could also see return path ingress and noise (Figure 30).

The 9580 series products evolved over time into the 9581 series. Trilithic developed the 860 DSP field meter to (eventually) receive downstream sweep, which also used the SST method for upstream testing.

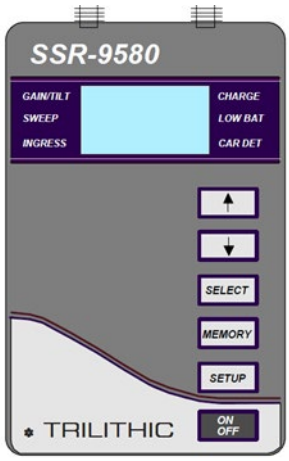

Figure 28 - Trilithic SSR-9580 (graphic from Trilithic "9580 Return Alignment System Operation Manual," courtesy of Viavi Solutions).

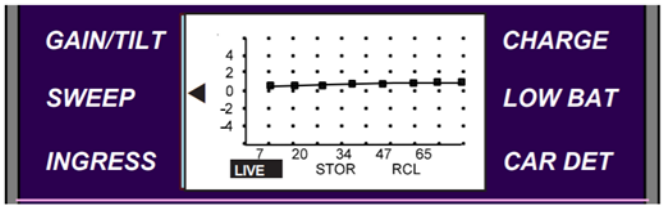

Figure 29 - Trilithic SSR-9580 upstream frequency response display (graphic from Trilithic "9580 Return Alignment System Operation Manual," courtesy of Viavi Solutions).

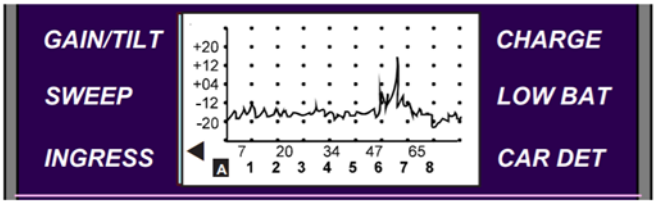

Figure 30 - Upstream ingress display from Trilithic SSR-9580 field unit (graphic from Trilithic "9580 Return Alignment System Operation Manual," courtesy of Viavi Solutions).

14. Return path alignment using portable oscillators

Another method was commonly used for aligning and testing the upstream. Here, too, it wasn't true sweep, but more of a visually-connect-the-dots approach. A company called Viewsonics (not the same company that makes computer equipment) manufactured a variety of cable-related products, among them small battery-operated CW carrier oscillators. One model, the VSOSC-2F Dual Frequency Oscillator, generated a pair of CW carriers at fixed frequencies such as 5 MHz and 30 MHz (frequencies determined when the product was ordered). Their VSHSS-7-42 Harmonic Signal Source produced CW carriers in the upstream at 7 MHz, 14 MHz, 21 MHz, 28 MHz, 35 MHz, and 42 MHz.

A tech would connect the signal generator to a tap or amplifier test point. The coarse frequency response could be determined when another tech observed the carriers in the headend or elsewhere in the network using a spectrum analyzer (a variation of the spectrum analyzer approach that could be used by just one tech is described below). Figure 31 shows two carriers from the VSOSC-2F, and Figure 32 shows multiple carriers from the VSHSS-7-42.

Applied Instruments was another company that offered CW carrier sources for upstream frequency response testing.

Figure 31 - Return path alignment carriers at 5 MHz and 30 MHz from a Viewsonics VSOSC-2F Dual Frequency Oscillator (photo courtesy of Jonathan Jurta, Atlantic Broadband).

Figure 32 - Return path alignment carriers at 7 MHz, 14 MHz, 21 MHz, 28 MHz, 35 MHz, and 42 MHz from a Viewsonics VSHSS-7-42 Harmonic Signal Source (photo courtesy of Jim Kuhns, CommScope).

A spectrum analyzer in the headend could support one-person operation, too. Here, the analyzer was connected to a suitable upstream test point, and the received CW carriers displayed on the analyzer's screen. A small TV camera was pointed at the screen, and the video output of the TV camera connected to a downstream TV modulator (alternatively, the video output from the analyzer – if equipped – was connected directly to the modulator's video input). The "spectrum analyzer channel" was usually carried at the upper end of the downstream spectrum. The field tech, who was operating the portable CW carrier generator, would tune a portable TV set to the spectrum analyzer channel, and look at the CW carriers on his TV. From that he could see the coarse upstream response as it appeared in the headend, and make adjustments in the field as necessary. The spectrum analyzer channel and portable TV combo also was used to troubleshoot upstream ingress.

15. Contemporary sweep equipment

VeEX and Viavi Solutions still manufacture and sell sweep equipment. Both of these manufacturers' products support forward and reverse sweep.

15.1. VeEX

Current sweep technology from VeEX operates largely in the same manner as legacy equipment: a combination of CaLan sweep technology, combined with "in-service sweep" to measure existing channels. The 3010H+, shown in Figure 33, supports forward sweep up to 1.8 GHz, and return sweep up to 204 MHz. The 3010H+ is compatible with the company's CX380s-D3.1; a soon-to-be released product called CX380C; and legacy CM3800 and CM2800 instruments (the latter two are limited to 1 GHz sweep). The sweep product line includes remote control features, along with the ability to remotely store and analyze sweep data collected in the field using the company's VeEX VeSion™ Cloud-Based One System Platform.

Figure 33 - VeEX 3010H+ sweep transmitter/receiver (courtesy of VeEX).

Distributed access architecture (DAA) technology such as remote PHY (R-PHY) uses digital optical links between the headend and node, so there is no RF transport available in the optical path. That limitation affects traditional sweep. To address this, VeEX developed the 3010F+ ("field"), in which the traditional headend- or hub-located forward sweep transmitter/return sweep receiver functionality is implemented in a portable field unit. The 3010F+ is used at the R-PHY node and simply plugs into existing RF test points, allowing sweep to be performed as usual. As DAA deployments become more widespread, VeEX is developing a more advanced 3010S+ ("server") platform that would be installed in the headend or hub to support R-PHY sweep operation with existing field meters.

15.2. Viavi

The company's ONX/SCU products support a downstream sweep frequency range to 1,218 MHz and 204 MHz in the upstream. The platform is compatible with existing Viavi sweep equipment (SDA-55xx, DSAM), and OneExpert field meters.

Figure 34 - Viavi SCU-1800 sweep control unit (courtesy of Viavi Solutions).

A 1RU sweep control unit (SCU-1800, shown in Figure 34) with 16 switchable return sweep ports reduces headend combining requirements, improving noise performance, and allowing sweep receivers to be consolidated. The sweep control unit is remotely or locally configurable and the interface is accessible via Ethernet/Internet/Intranet and browser. Improved pulse generation performance provides narrower

sweep pulses enabling insertion between active carriers. Upstream frequency response testing is done using either injected sweep points or Sweepless Sweep (the latter is based upon response derived from pre-equalization coefficients).

Viavi's sweep system has been integrated to work with several vendors' DAA technology. Narrowband digital forward (NDF) and narrowband digital return (NDR) transport telemetry signals between field units and the headend/hub. Downstream sweep is done using Sweepless Sweep, and upstream sweep uses triggered spectrum capture in the R-PHY node to transmit field-unit-generated sweep point data back to the headend/hub. Orchestration and communications are handled by the Viavi XPERTrak R-PHY/CCAP Interface (RCI) software and XPERTrak server. From the perspective of technicians in the field, sweep operation is essentially the same as if dedicated RF paths existed between the headend/hub and R-PHY nodes.

16. Spectrum displays of frequency response

The industry also uses various spectrum display methods to help characterize downstream frequency response, as well as in-channel frequency response derived from adaptive equalizer coefficients. The following sections briefly describe these methods.

17. Spectrum analyzers

Spectrum analyzers – along with spectrum monitoring devices similar to spectrum analyzers – graphically display magnitude (amplitude) in the vertical axis and frequency in the horizontal axis, and can be used to observe a cable network's RF spectrum and provide an approximation of frequency response. Figure 35 shows a screen shot from an old Hewlett-Packard 8590-series spectrum analyzer connected to an in-home subscriber drop. In the figure, one can discern a slight downward tilt from low-to-high frequency, and a non-flat response "hump" in the upper part of the spectrum. The apparent suckouts (notches) in the response are parts of the spectrum with no signals present.

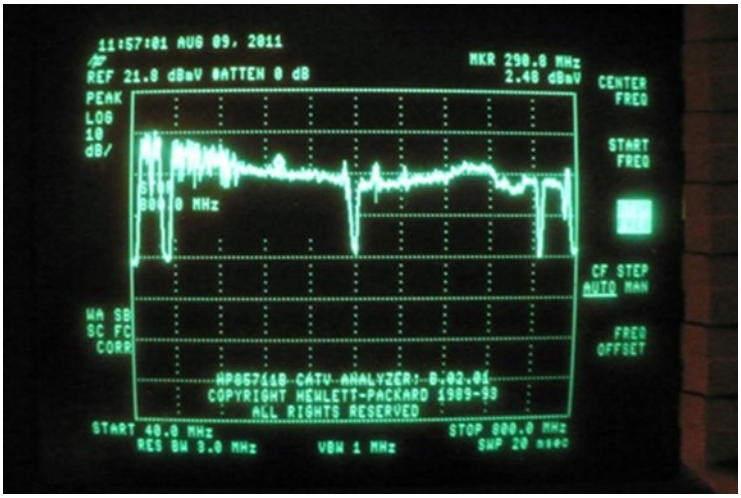

Figure 35 - Spectrum analyzer display of downstream RF spectrum at the end of a subscriber drop.

18. Field meters

Figure 36 is a screen shot from a Viavi OneExpert meter, showing a “ChannelCheck” graph of RF signal level-versus-frequency. This was captured in a residential subscriber drop and allows one to see the coarse frequency response. The tall blue spike that sticks up a little to the right of center represents a CW carrier whose signal level is about 6 dB higher than the digital channel power of the surrounding SC-QAM signals (the wide pinkish-colored block at the upper edge of the spectrum represents a 96 MHz-wide OFDM signal).

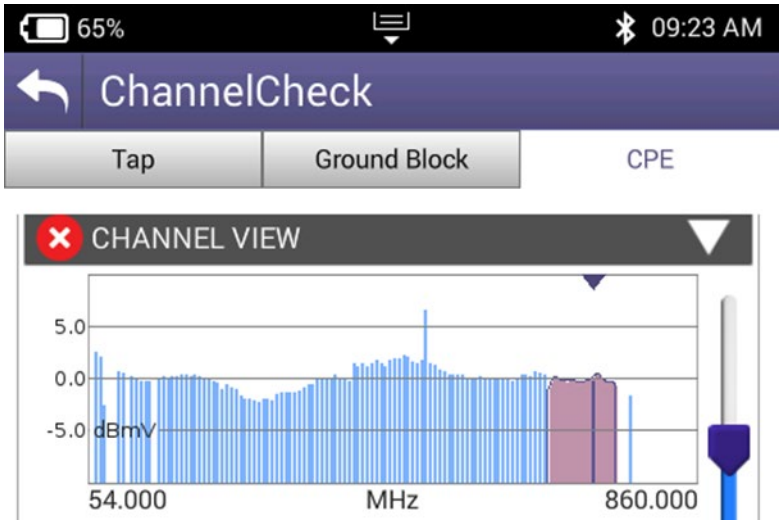

Figure 36 - Viavi OneExpert "ChannelCheck" display of RF signal level-versus-frequency.

19. Full band capture

Many DOCSIS 3.0 cable modems (and all DOCSIS 3.1 modems) include a feature known as full band capture, in which internal circuitry can be used to capture RF signal power-versus-frequency data. That data can be displayed graphically similar to a spectrum analyzer screen shot, giving the equivalent of a spectrum analyzer-like device in all homes equipped with FBC-capable modems. Figure 37 is an FBC display showing a downstream spectrum that has relatively flat frequency response. The FBC display also shows the presence of some ingress (circled in red).

Figure 37 - Full band capture display showing relatively flat frequency response. Ingress is also visible (circled in red). Graphic courtesy of Comcast.

Figure 38 is another example of an FBC display, this one showing several frequency response impairments.

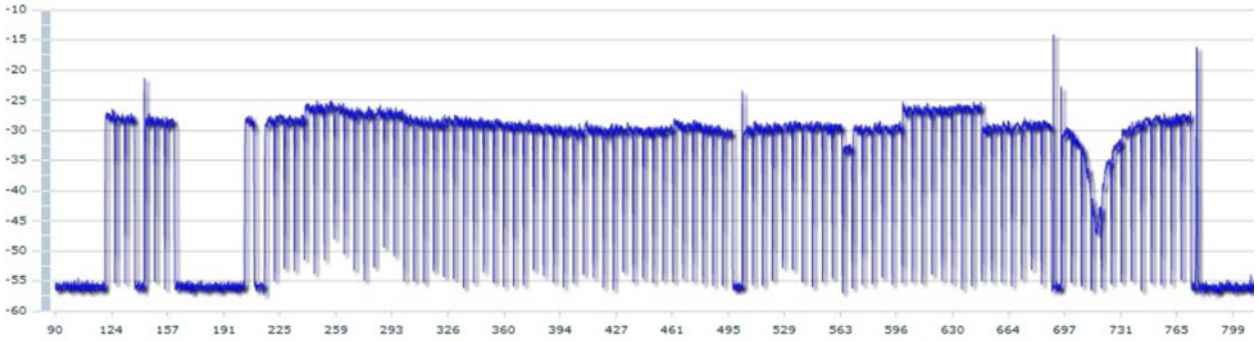

Figure 38 - Another cable modem FBC display. This example shows several frequency response problems. Graphic courtesy of Comcast.

Proactive network maintenance (PNM) tools that incorporate special signature identification algorithms can automatically identify FBC frequency response issues such as amplitude ripple (standing waves), suckouts, peaking, excessive tilt, rolloff, adjacency, and so on.

20. In-channel frequency response derived from adaptive equalizer coefficients

It is possible to derive in-channel frequency response from a cable modem's adaptive equalizer coefficients. Some field instruments that use embedded cable modem silicon support this capability for downstream SC-QAM signals, as shown in the center graphic of Figure 39. Adaptive equalizer-derived ICFR is limited to the signal's symbol rate bandwidth – for instance, 5.36 MHz for a 6 MHz-wide 256-QAM signal.

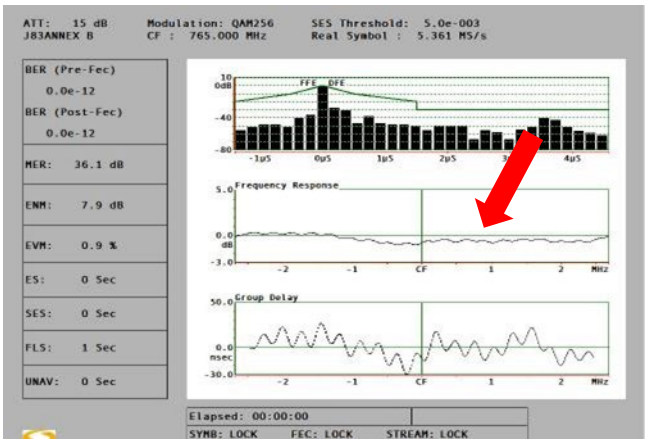

Figure 39 - In-channel frequency response (arrow) for a downstream SC-QAM signal on CTA channel 119 (765 MHz center frequency).

As well, in-channel frequency response can be derived from cable modem upstream adaptive pre-equalization coefficients (the same symbol rate bandwidth limitation applies). To better understand this, the following section briefly discusses the operation of adaptive equalizers.

21. Adaptive equalizer overview

An adaptive equalizer is a digital circuit that compensates for a digitally modulated signal's in-channel complex frequency response impairments. An adaptive equalizer can compensate for in-channel amplitude- and phase-versus-frequency impairments. Adaptive equalization is used in both downstream and upstream data transmission in cable networks.

The adaptive equalizer, which is part of the QAM demodulator silicon in digital set-tops, cable modems, CMTS upstream receivers, and some test equipment, uses sophisticated algorithms to derive coefficients for an equalizer solution "on the fly" – in effect, creating a digital filter with essentially the opposite complex frequency response of the impaired channel. Because the adaptive equalizer's complex frequency response is essentially a mirror image of the impaired channel's complex frequency response, it cancels out most or all of the degraded in-channel frequency response that is affecting the digital signal – within the limits of the adaptive equalizer's capabilities, of course. (It's important to note that at high signal-to-noise ratio (E_S/N_0) the adaptive equalizer will synthesize the opposite response of the channel. At lower SNR doing so would cause noise enhancement, so a compromise solution is derived.)

Since an adaptive equalizer creates a digital filter with the opposite frequency response of the channel, that equalizer's frequency response can provide an indication of what the channel's response looks like. Thus, one can derive an in-channel frequency response plot (actually the adaptive equalizer's frequency response) from the equalizer coefficients. This method has been a core part of proactive network maintenance tools for many years, in particular for determining in-channel frequency response of the cable network's active upstream DOCSIS channels.

DOCSIS 1.1 and later cable modems are capable of equalizing – or more accurately, pre-equalizing – their transmitted upstream signals. DOCSIS 1.1 modems support 8-tap upstream pre-equalization, while DOCSIS 2.0 and later modems support 24-tap upstream pre-equalization for SC-QAM signals. Why pre-equalize in the modem rather than at the CMTS?

First, the path between each modem and the CMTS is unique. Pre-equalization allows most of the adaptive equalization to be done by the modem before upstream transmission, rather than relying upon the CMTS to do all of the work. A cable modem has no way of knowing the condition of the channel between its upstream transmitter output and the CMTS's input. The modem can't "see" the channel through which the upstream digitally modulated signal is transmitted, so how can a cable modem correctly pre-equalize a transmitted upstream signal?

The cable modem transmits station maintenance bursts to the CMTS, which uses the preamble of the unequalized (RNG-REQ) station maintenance message as a "training signal" for the equalization process. The CMTS's upstream burst receiver includes an adaptive equalizer that derives coefficients based on the channel impairment(s) affecting the received signal. The CMTS transmits the derived equalizer coefficients to the modem in a RNG-RSP MAC message. The cable modem uses the equalizer coefficients in its upstream adaptive equalizer to pre-equalize or pre-distort the transmitted signal, so that when it is received by the CMTS it will, in theory, be unimpaired.

The pre-equalization coefficients can be used for more than the pre-equalization process just described. One can derive in-channel frequency response from those coefficients, and display that frequency response graphically, as shown in Figure 40. Technically speaking, the derived ICFR is actually that of the adaptive pre-equalizer rather than the channel, so it shows the inverse response of the channel (actually the channel's symbol rate bandwidth – for instance, 5.12 MHz for a 6.4 MHz-wide SC-QAM signal).

Some cable operators use PNM tools that can identify upstream ICFR signatures with out-of-tolerance conditions, whether for individual cable modems (caused by individual drop problems) or groups of modems (caused by distribution network problems common to the affected modems).

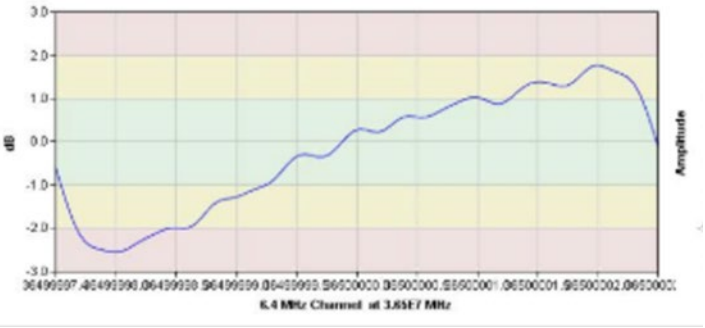

Figure 40 - ICFR derived from pre-equalization coefficients for an SC-QAM signal carried at the upper end of the return spectrum. The channel's response is the inverse of what is shown here, so is actually tilted downwards left-to-right. Graphic courtesy of Comcast.

Figure 41, Figure 42, Figure 43, and Figure 44 show the ICFR derived from pre-equalization coefficients from four upstream channels, centered at 36.5 MHz, 30.1 MHz, 23.7 MHz, and 17.3 MHz respectively. It's clear that each channel's ICFR is degraded by standing waves (amplitude ripple).

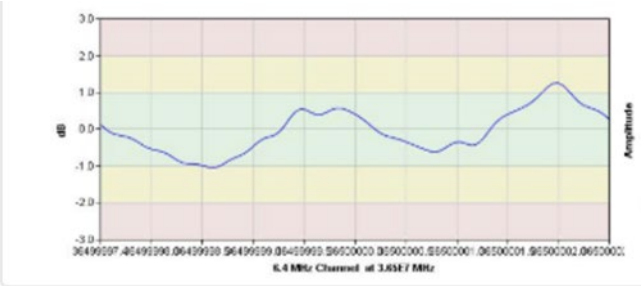

Figure 41 - ICFR for an upstream SC-QAM signal centered at 36.5 MHz. Note the presence of standing waves (amplitude ripple). Graphic courtesy of Comcast.

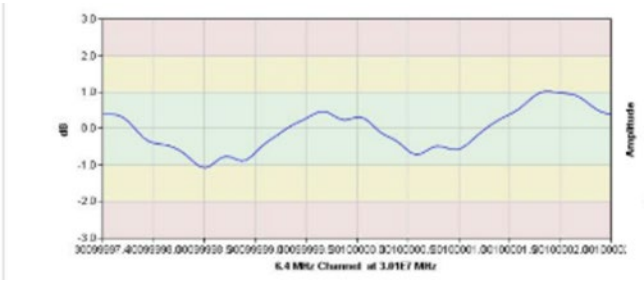

Figure 42 - ICFR for an upstream SC-QAM signal centered at 30.1 MHz in the same return spectrum as the previous figure. Graphic courtesy of Comcast.

Figure 43 - ICFR for an upstream SC-QAM signal centered at 23.7 MHz. Graphic courtesy of Comcast.

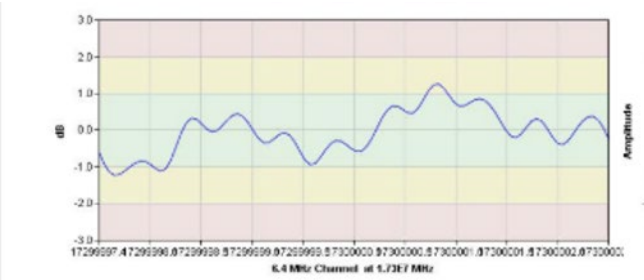

Figure 44 - ICFR for an upstream SC-QAM signal centered at 17.3 MHz. Graphic courtesy of Comcast.

Figure 45 shows the four ICFR graphs spliced together, giving an indication of the frequency response across the occupied part of the upstream spectrum. This can be a powerful tool for characterizing the health of the upstream, although it does not show the response of that part of the spectrum without active DOCSIS signals. Likewise, there is a small gap in the response between each SC-QAM signal, because the ICFR plots are, as mentioned previously, limited to each signal's symbol rate bandwidth. Using pre-equalization coefficient-derived ICFR for upstream alignment is limited from a real-time perspective, because of the relatively slow update rate (typically tens of seconds).

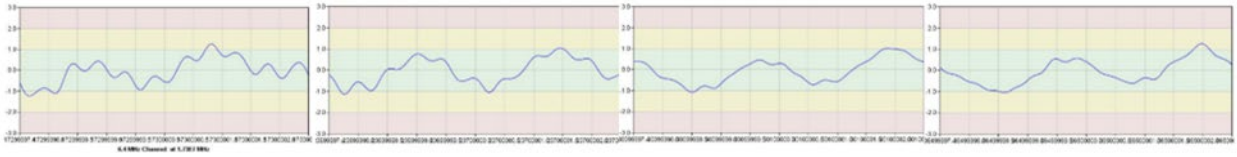

Figure 45 - The ICFR graphs from the previous four figures spliced together to show the frequency response across the spectrum occupied by active DOCSIS signals.

Some test equipment vendors incorporate the use of pre-equalization coefficient-derived ICFR technology in their portable test instruments; Figure 46 shows an example. This particular implementation supports data capture from the same cable modem reference frequency response and overlaying a subsequent capture at a different test point to validate upstream unity gain and tilt.

Figure 47 shows another example of the use of pre-equalization coefficient-derived ICFR technology.

Figure 46 - Example of commercial implementation of upstream active spectrum frequency response derived from pre-equalization coefficients. This screen shot shows a captured reference (red traces) and a response trace from another test point affected by an impairment (yellow traces). Graphic courtesy of Deviser Instruments.

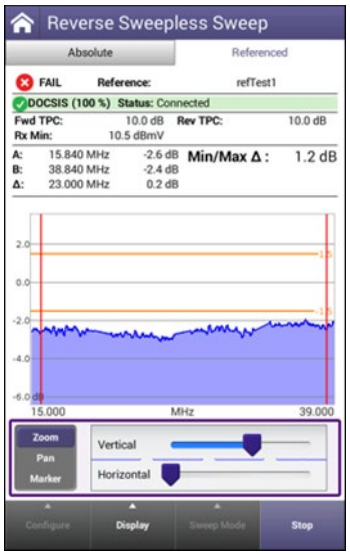

Figure 47 - Another example of commercial implementation of upstream active spectrum frequency response derived from pre-equalization coefficients. Graphic courtesy of Viavi Solutions.

22. Conclusion

Characterizing and maintaining proper frequency response has for decades been among the tools used by cable operators to ensure optimum performance of their networks. As mentioned in the introduction to this document, cable network performance is dependent upon a variety of factors. Many types of problems and impairments can be identified by what has long been called broadband sweeping. While some operators have reduced or eliminated sweeping as modern HFC architectures bring fiber closer to the home and reduce the amount of coax plant, frequency response-related problems still occur. Without an adequate means to characterize a network's frequency response, some of those problems can remain hidden until they impact service to subscribers. As long as RF is present in cable networks, sweeping should be considered an important part of network maintenance.

23. Abbreviations and Definitions

23.1. Abbreviations

1RU	one rack unit
AGC	automatic gain control
Ch.	channel
CMTS	cable modem termination system
CNR	carrier-to-noise ratio
CTA	Consumer Technology Association
CW	continuous wave
DAA	distributed access architecture
dB	decibel
DOCSIS	Data-Over-Cable Service Interface Specifications

DUT	device under test
E_S/N_0	energy-per-symbol to noise-density ratio
FBC	full band capture
GHz	gigahertz
HFC	hybrid fiber/coax
ICFR	in-channel frequency response
MAC	media access control
MHz	megahertz
NDF	narrowband digital forward
NDR	narrowband digital return
NTSC	National Television System Committee
OFDM	orthogonal frequency division multiplexing
PNM	proactive network maintenance
QAM	quadrature amplitude modulation
RF	radio frequency
RNG-REQ	ranging request
RNG-RSP	ranging response
R-PHY	remote physical layer (remote PHY)
SC-QAM	single carrier quadrature amplitude modulation
SNR	signal-to-noise ratio
TV	television
VITS	vertical interval test signal

23.2. Definitions

balance	A cable network alignment method using two carriers or signals – one at the low end of the RF spectrum and the other at the high end of the RF spectrum.
complex frequency response	A measure of magnitude- and phase-versus-frequency of a device or network under test.
frequency response (*cable industry common usage*)	A measure of the overall gain variation of a cable network or an individual channel as a function of frequency – that is, magnitude (or amplitude)-versus-frequency.
in-channel frequency response (ICFR)	A measure of magnitude- and/or phase-versus-frequency of an individual upstream or downstream channel.
sweep	A method of cable network frequency response characterization, in which an injected test signal's frequency is varied continuously or stepped across a frequency range of interest while maintaining a constant amplitude. A receiver synchronized to the test signal's transmitter captures the test signal and displays a plot of its amplitude-versus-frequency.
sweep point	A special test signal injected at pre-defined frequencies for use as a reference when characterizing frequency response.

24. Bibliography and References

- Acterna SDA Series Stealth Digital Analyzer Operation Manual, 6510-00-0442, Rev F August 2004
- CaLan 1776/1777 Integrated Sweep/Spectrum Analyzer Systems product data sheet
- JDSU Application Note: Using JDSU's Family of SDA Sweep for Reverse and Balance, 2006
- Jerrold Technical Seminar Manual (undated, from 1970s)
- SCTE Measurement Recommended Practices for Cable Systems, Fourth Edition, ©2012
- Tektronix NTSC Video Measurements Primer, August 2003
- Trilithic 9580 Return Alignment System Operation Manual, P/N 0010157004, June 2004
- Trilithic 9580 SSR/EU Operation Manual, P/N P/N 0010203000, January 2004
- VeEX CaLan 3010H+ User Manual, D07-00-108P-RevA00, ©2017
- VeEX VePAL CX-380/CX-380-D3 Advanced CATV System Analyzer User Manual, D07-00-108P-RevA00, ©2006-2012
- Viavi Digital Service Analysis Meter, DSAM-6300 data sheet, 2015

25. Appendix

25.1. Frequency response examples

This section of the document includes screen shots of broadband sweep frequency response examples seen in the field.

25.1.1. Normalized frequency response reference

Usually captured, normalized, and stored by the sweep receiver at the node or first amplifier output. Subsequent measurements are compared to the reference by the sweep receiver, and the displayed difference shows the frequency response to that point.

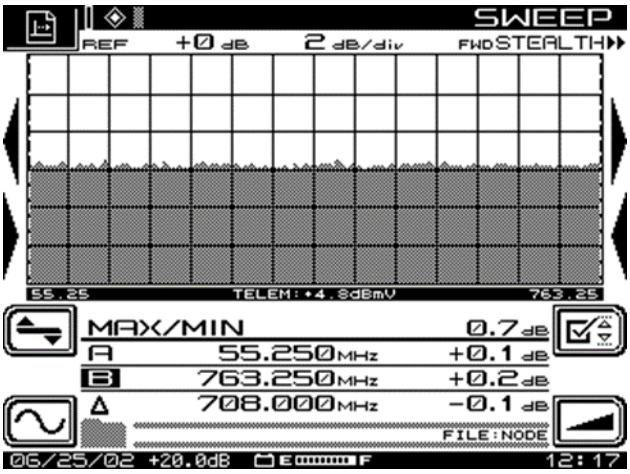

Figure 48. Normalized frequency response reference (courtesy of Viavi Solutions).

25.1.2. Suckout

A notch in the frequency response, which can affect one to several adjacent channels. Caused by loose modules, module covers, printed circuit boards, poor grounding, and similar problems inside of active or passive device housings. Can also be caused by repetitive, regularly spaced impedance discontinuities in coaxial cable.

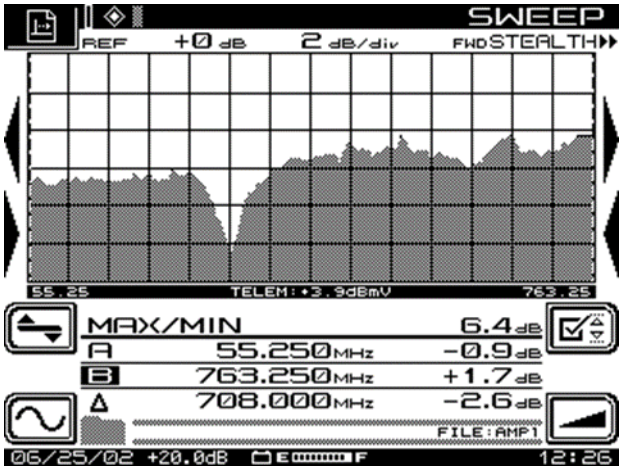

Figure 49. Frequency response suckout (courtesy Viavi).

Figure 50. Another example of a frequency response suckout (courtesy VeEX).

25.1.3. Standing waves (amplitude ripple)

Scalloped sinusoidal or sinusoidal-like shape in the frequency response, caused by one or more impedance mismatches in the signal path. The signal reflected by an impedance mismatch interacts with the incident signal to produce a standing wave.

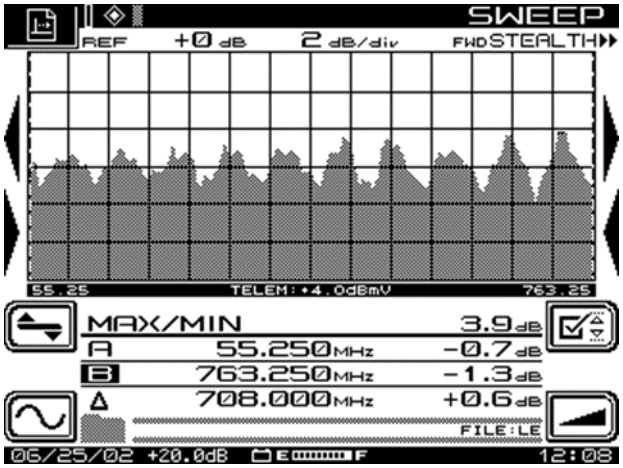

Figure 51. Standing wave (courtesy of Viavi Solutions).

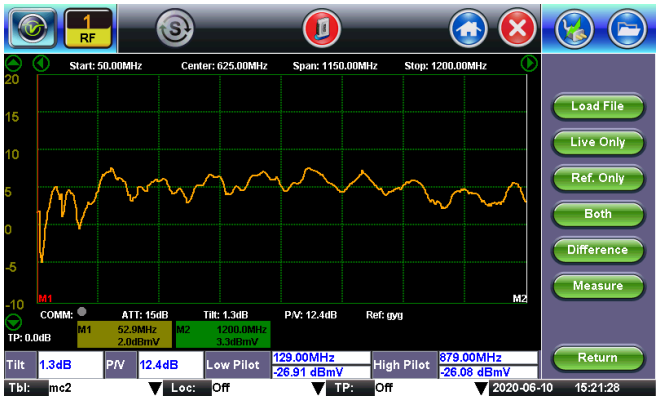

Figure 52. Another standing wave example (courtesy of VeEX).

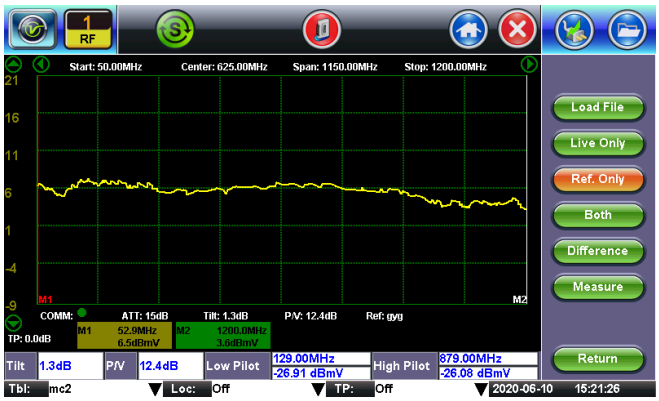

Figure 53. Same swept spectrum as Figure 52, but without the impedance mismatch that caused the standing wave (courtesy of VeEX).

25.1.4. Negative tilt

Typical frequency response seen at and near ends-of-line locations, but can occur as a result of active device misalignment or failure, or excessive higher frequency loss caused by cable or equipment damage.

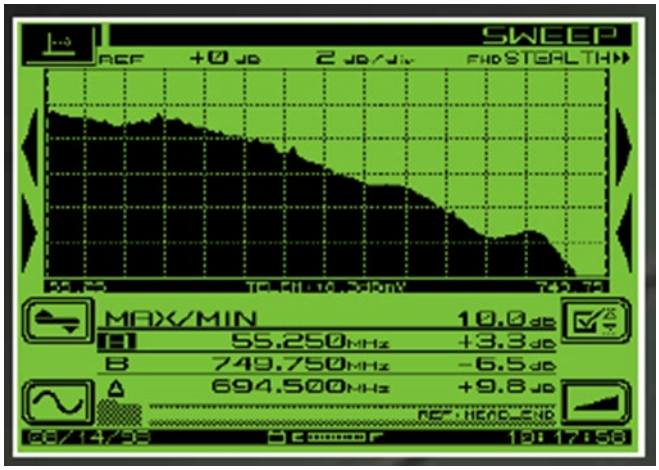

Figure 54. Negative tilt (courtesy of Viavi Solutions).

25.1.5. Positive tilt

Typical frequency response seen at the output of a node or amplifier.

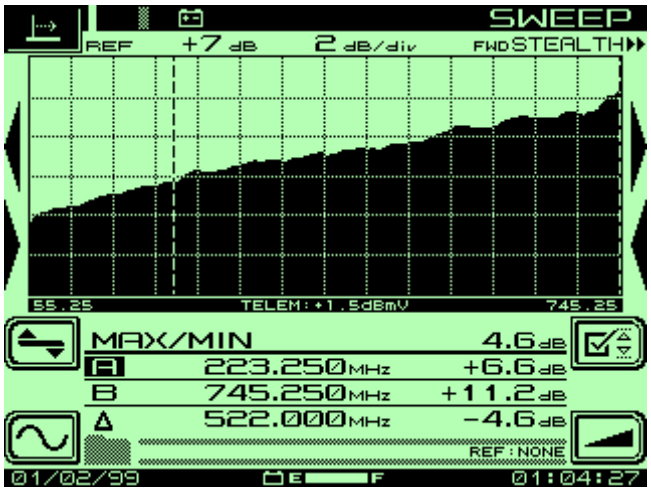

Figure 55. Positive tilt (courtesy of Viavi Solutions).

25.1.6. Damaged cable

This example was observed in the field, and was found to be caused by a cracked cable shield about 180 feet prior to the input of an amplifier.

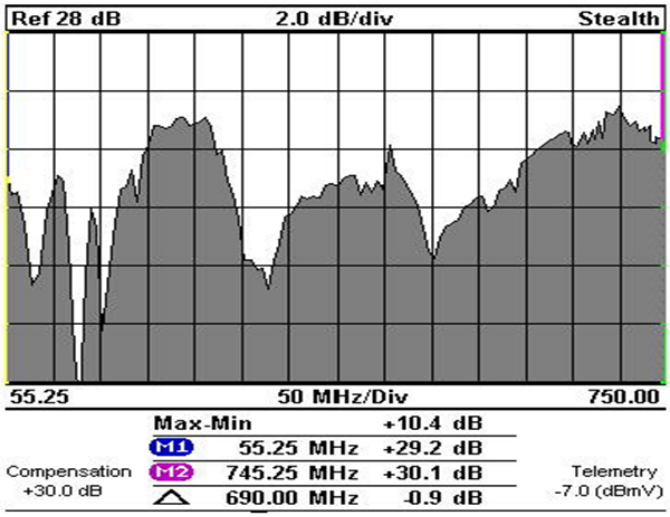

Figure 56. Cracked cable shielding caused this degraded frequency response (courtesy of Viavi Solutions).

25.1.7. Mold spike suckout

A frequency response suckout caused by the repetitive spacing of an impedance discontinuity in first generation MC^2 coaxial cable. The so-called mold spike was related to the physical dimensions of the mold used to place groups of disks over the cable's center conductor during manufacture. The spacing between groups of disks caused a structural return loss (SRL) spike in the 500 MHz to 600 MHz range, which in turn could result in a suckout in the frequency response at the same frequency. The mold was later redesigned to place the SRL spike above 1 GHz. Note: MC^2 cable is no longer available, but it still exists in some cable networks.

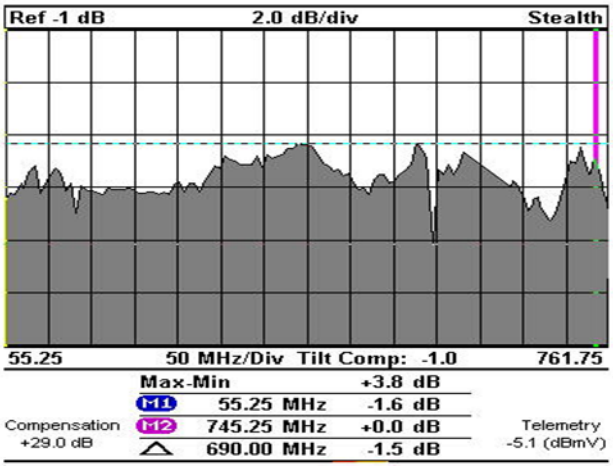

Figure 57. So-called mold spike suckout (courtesy of Viavi Solutions).

25.1.8. Low end rolloff

Excess attenuation at the low end of the downstream spectrum, typically caused by a loose center conductor seizure screw in an active or passive device. Can also be caused by a defective plug-in accessory or diplex filter.

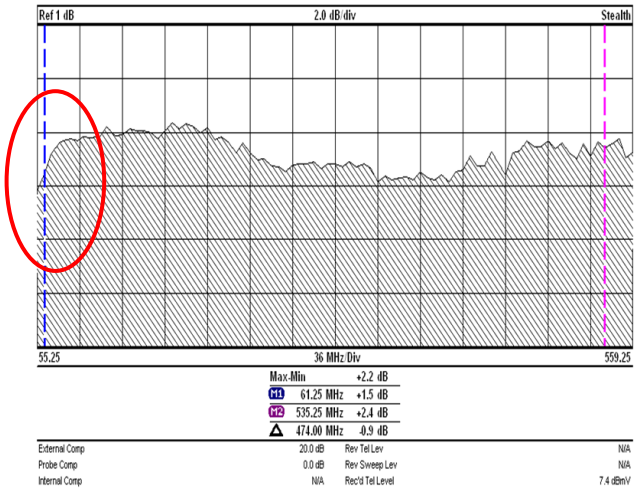

Figure 58. Low-end rolloff (courtesy of Viavi Solutions).

Figure 59. Another example of low-end rolloff (courtesy of VeEX).

SCTE • ISBE
STANDARDS

NETWORK
OPERATIONS